Electronic Supplementary Material (ESI) for ChemComm.

Electronic Supporting Information

Self-Assembly of a Porous Metallo-[5] Rotaxane

Kevin Kei Gwan Wong, Nadia Hoyas Pérez, Andrew J. P. White and James E. M. Lewis*

Department of Chemistry, Imperial College London, Molecular Sciences Research Hub,

80 Wood Lane, London W12 0BZ, UK

*james.lewis@imperial.ac.uk

Contents

General Experimental

Synthesis: Unless otherwise stated, all reagents, including anhydrous solvents, were purchased from commercial sources and used without further purification. $CDCl_3$ and NEt_3 were stored over 4 Å molecular sieves prior to use. All reactions were carried out under an atmosphere of N_2 using degassed, anhydrous solvents unless otherwise stated. Petrol refers to the fraction of petroleum ether boiling in the range 40-60 °C. Analytical TLC was performed on pre-coated silica gel plates (0.25 mm thick, 60F254, Merck, Germany) and observed under UV light. EDTA solution refers to a 0.1 M solution of EDTA-Na_2 in 3% $NH_{3(aq)}$.

Analysis: NMR spectra were recorded on Bruker AV400 or AV500 instrument, at a constant temperature of 300 K. Chemical shifts are reported in parts per million from low to high field and referenced to residual solvent. Standard abbreviations indicating multiplicity were used as follows: m = multiplet, quint = quintet, q = quartet, t = triplet, d = doublet, s = singlet, app. = apparent, br. = broad. Signal assignment was carried out using 2D NMR methods (HSQC, HMBC, COSY, NOESY) where necessary. In the case of some signals absolute assignment was not possible. Here indicative either/or assignments (e.g. H_A/H_B for H_A or H_B) are provided. All melting points were determined using a hot stage apparatus and are uncorrected. Mass spectrometry was carried out by the Imperial College London, Department of Chemistry Mass Spectroscopy Service using Waters LCT Premier for HR-ESI-MS and Thermo Scientific Q-Exactive for tandem MS.

The following compound was synthesised according to a literature procedure:[1]

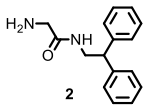

2

Synthetic Procedures

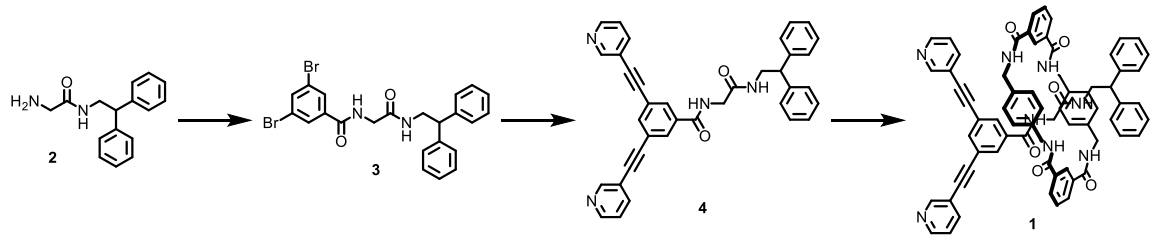

Synthesis of 3

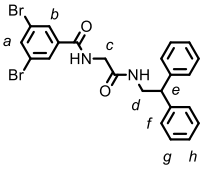

EDC (0.123 g, 0.642 mmol, 1 eq.) was added in small batches to a solution of 3,5-dibromobenzoic acid (0.180 g, 0.643 mmol, 1 eq.) and DMAP (0.079 g, 0.65 mmol, 1 eq.) in CH_2Cl_2 (20 mL) at rt. The reaction mixture was stirred for 10 min before **2** (0.164 g, 0.643 mmol, 1 eq.) was added as a solid. The reaction mixture was stirred at rt overnight then washed with 1 M $HCl_{(aq)}$ (3 × 10 mL), sat. aq. $NaHCO_3$ (3 × 10 mL) and brine (2 × 10 mL), dried ($MgSO_4$) and the solvent removed *in vacuo*. The crude material was purified by chromatography on silica (1:9 acetone/CH_2Cl_2) to afford **3** as a yellow foam (0.254 g, 0.453 mmol, 77%). M.p. 119-121 °C. ^{1}H NMR (400 MHz, $CDCl_3$) δ: 7.82 (d, J = 1.7 Hz, 2H, H_b), 7.80 (t, J = 1.7 Hz, 1H, H_a), 7.30-7.19 (m, 11H, H_f, H_g, H_h, H_{NH}), 6.23 (t, J = 5.5 Hz, 1H, H_{NH}), 4.18 (t, J = 8.0 Hz, 1H, H_e), 3.95-3.92 (m, 4H, H_c, H_d). ^{13}C NMR (101 MHz, $CDCl_3$) δ: 168.6, 165.0, 141.5, 137.3, 136.7, 129.3, 129.0, 128.1, 127.2, 123.4, 50.7, 44.0, 43.9. HR-ESIMS m/z = 514.9972 $[M+H]^+$ calc. 514.9970.

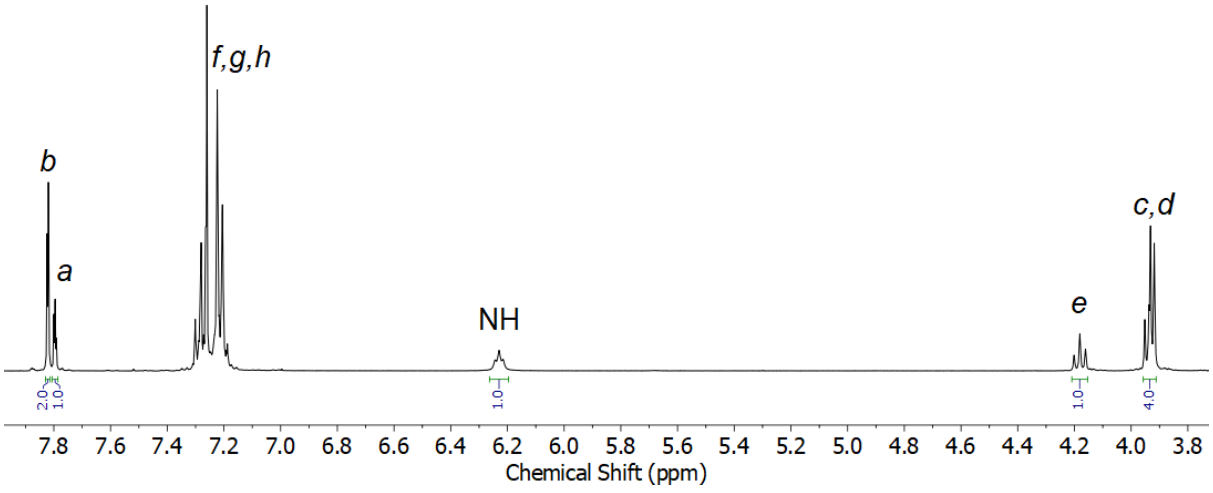

Figure S1 ^{1}H NMR ($CDCl_3$, 400 MHz) of **3**.

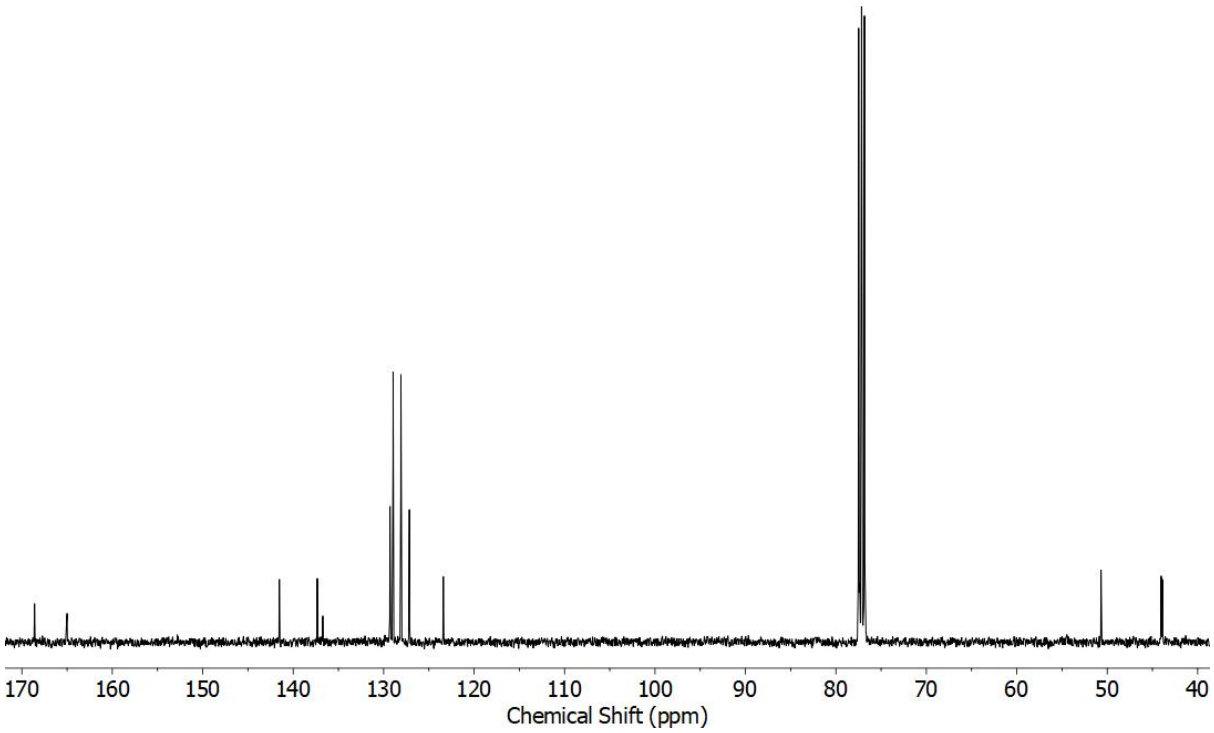

Figure S2 ^{13}C NMR ($CDCl_3$, 101 MHz) of **3**.

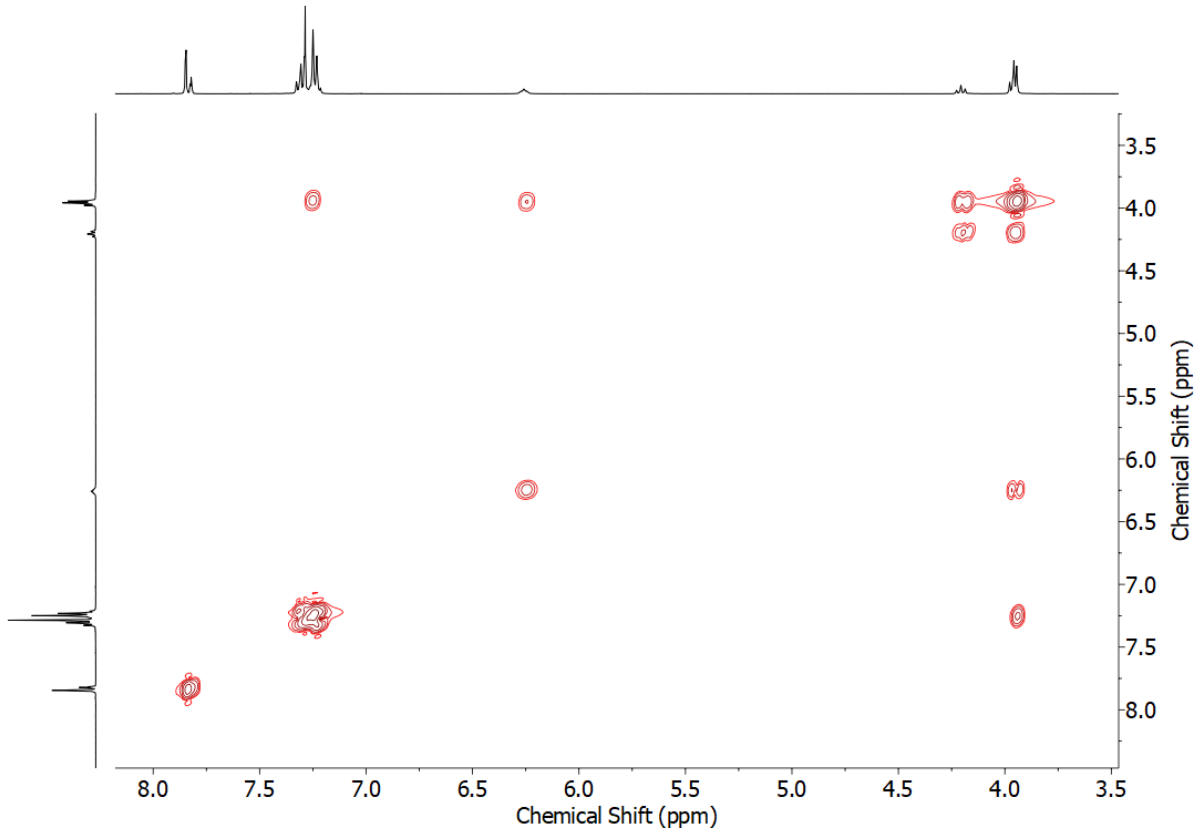

Figure S3 COSY NMR ($CDCl_3$) of **3**.

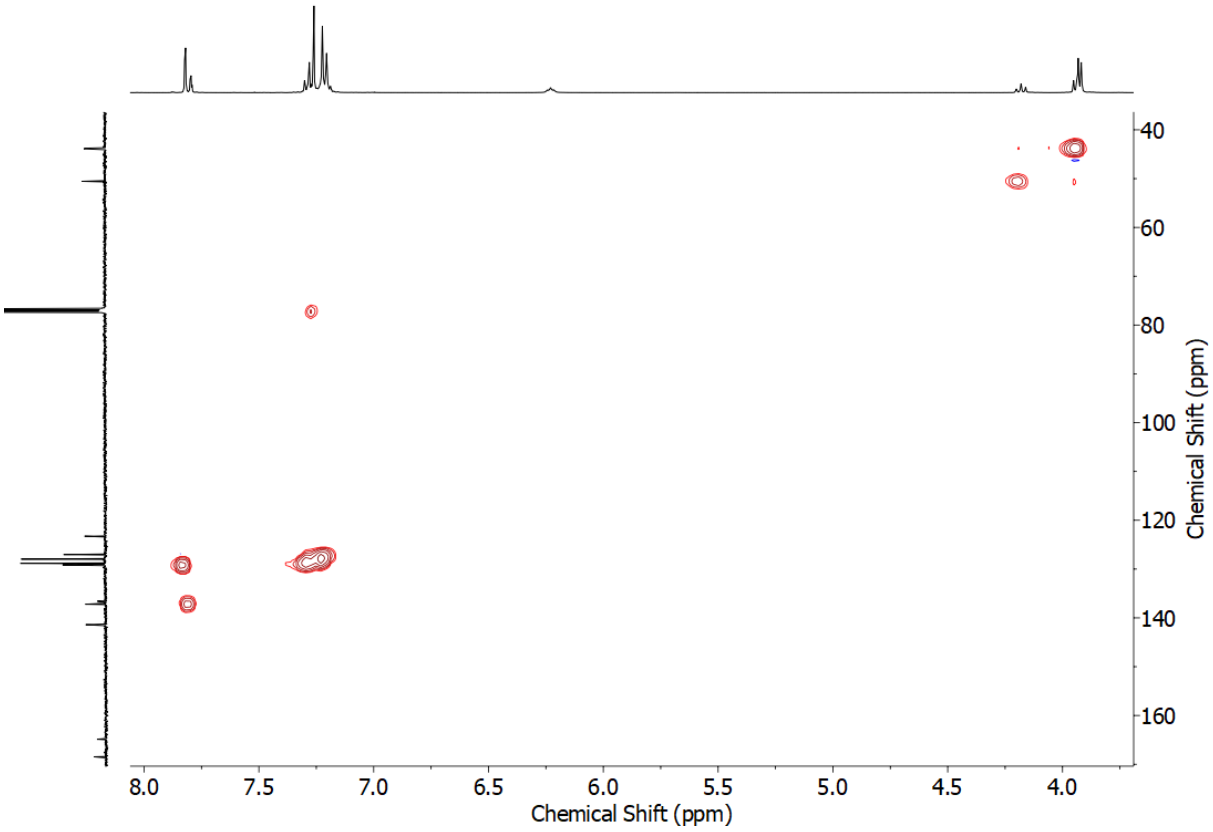

Figure S4 HSQC NMR ($CDCl_3$) of **3**.

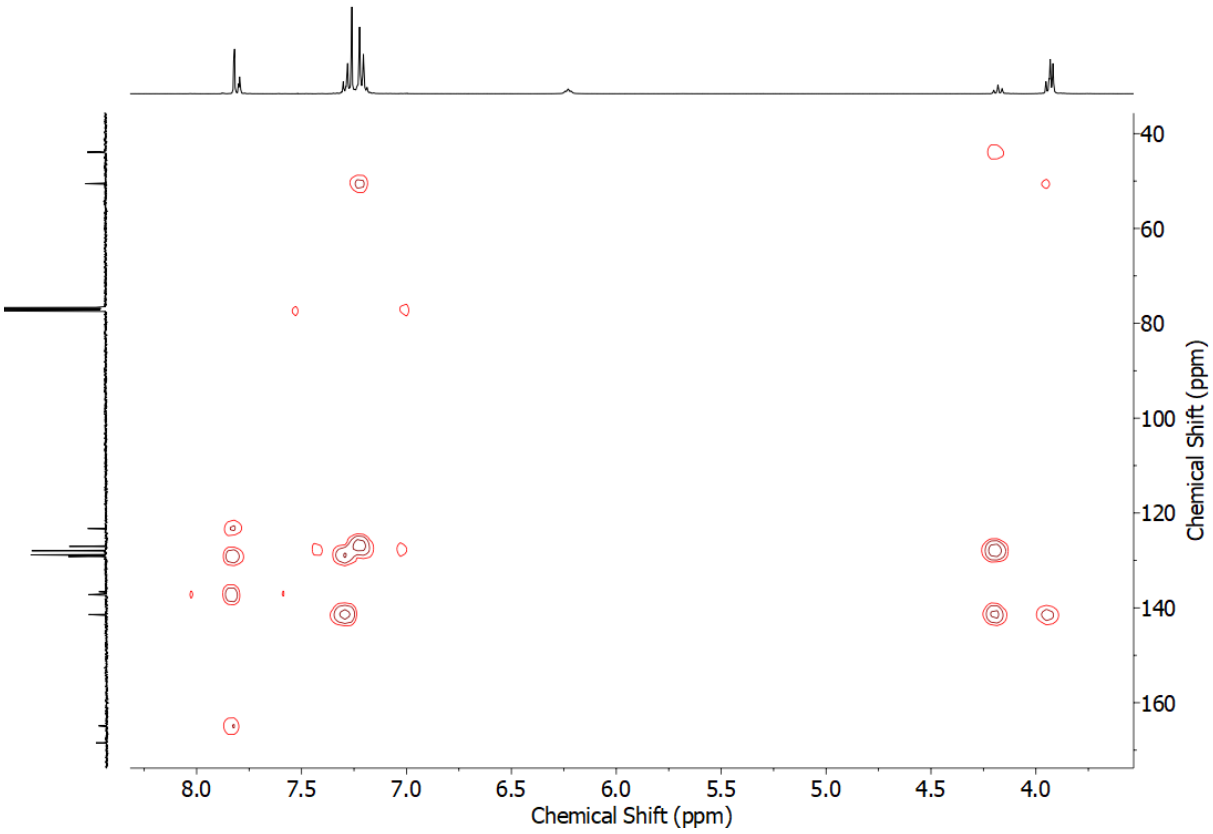

Figure S5 HMBC NMR ($CDCl_3$) of **3**.

Synthesis of 4

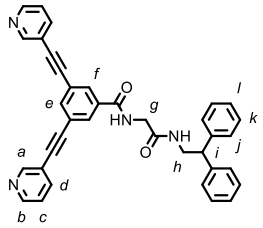

3 (0.142 g, 0.275 mmol, 1 eq.), 3-ethynylpyridine (0.085 g, 0.83 mmol, 3 eq.), $Pd(PPh_3)_2Cl_2$ (0.010 g, 0.014 mmol, 5 mol%), CuI (0.005 g, 0.03 mol, 10 mol%) were stirred at 80 °C in $^{i}Pr_2NH$ (10 mL) in a sealed vial for 16 h. EDTA solution (30 mL) was added and the aqueous phase extracted with CH_2Cl_2 (30 mL). The organic phase was washed with brine (2 × 10 mL), dried ($MgSO_4$) and the solvent removed *in vacuo*. The crude material was purified by chromatography on silica (1:4 acetone/CH_2Cl_2) to afford **4** as a brown solid (0.115 g, 0.205 mmol, 75%). M.p. 138-140 °C. ^{1}H NMR (400 MHz, $CDCl_3$) δ: 8.80 (d, *J* = 1.3 Hz, 2H, H_a), 8.60 (dd, *J* = 4.8, 1.5 Hz, 2H, H_b), 7.94 (d, *J* = 1.5 Hz, 2H, H_f), 7.86 (t, *J* = 1.5 Hz, 1H, H_e), 7.84 (app. dt, *J* = 7.9, 1.9 Hz, 2H, H_d), 7.35-7.20 (m, 13H, H_c, H_j, H_k, H_l, H_{NH}), 6.38 (t, *J* = 5.7 Hz, 1H, H_{NH}), 4.23 (t, *J* = 8.0 Hz, 1H, H_i), 4.03 (d, *J* = 5.0 Hz, 2H, H_g), 3.98 (dd, *J* = 8.1, 5.7 Hz, 2H, H_h). Diffusion coefficient (500 MHz, d_6-DMSO) *D*: 1.72 × 10^{-10} m^2s^{-1}. ^{13}C NMR (101 MHz, $CDCl_3$) δ: 168.6, 166.0, 152.4, 149.2, 141.6, 138.7, 137.4, 134.5, 130.5, 128.9, 128.1, 127.1, 123.8, 123.3, 119.9, 90.7, 87.9, 50.7, 44.1, 43.8. HR-ESI-MS m/z = 561.2287 $[M+H]^+$ calc. 561.2291.

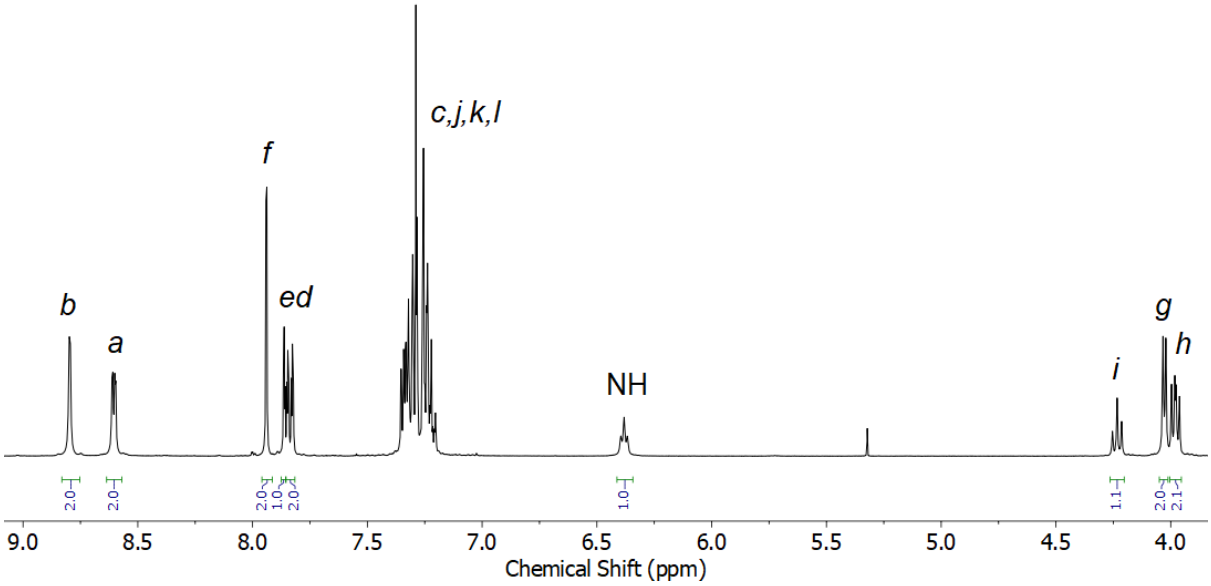

Figure S6 ^{1}H NMR ($CDCl_3$, 400 MHz) of **4**.

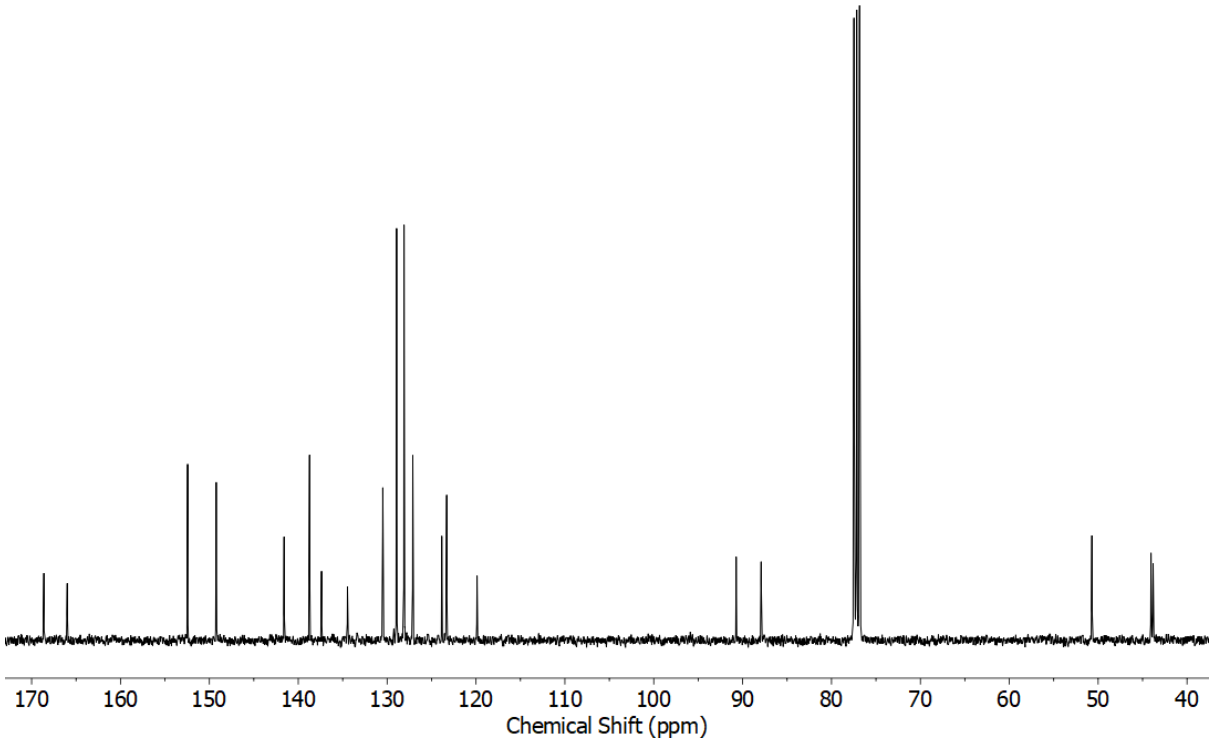

Figure S7 ^{13}C NMR ($CDCl_3$, 101 MHz) of **4**.

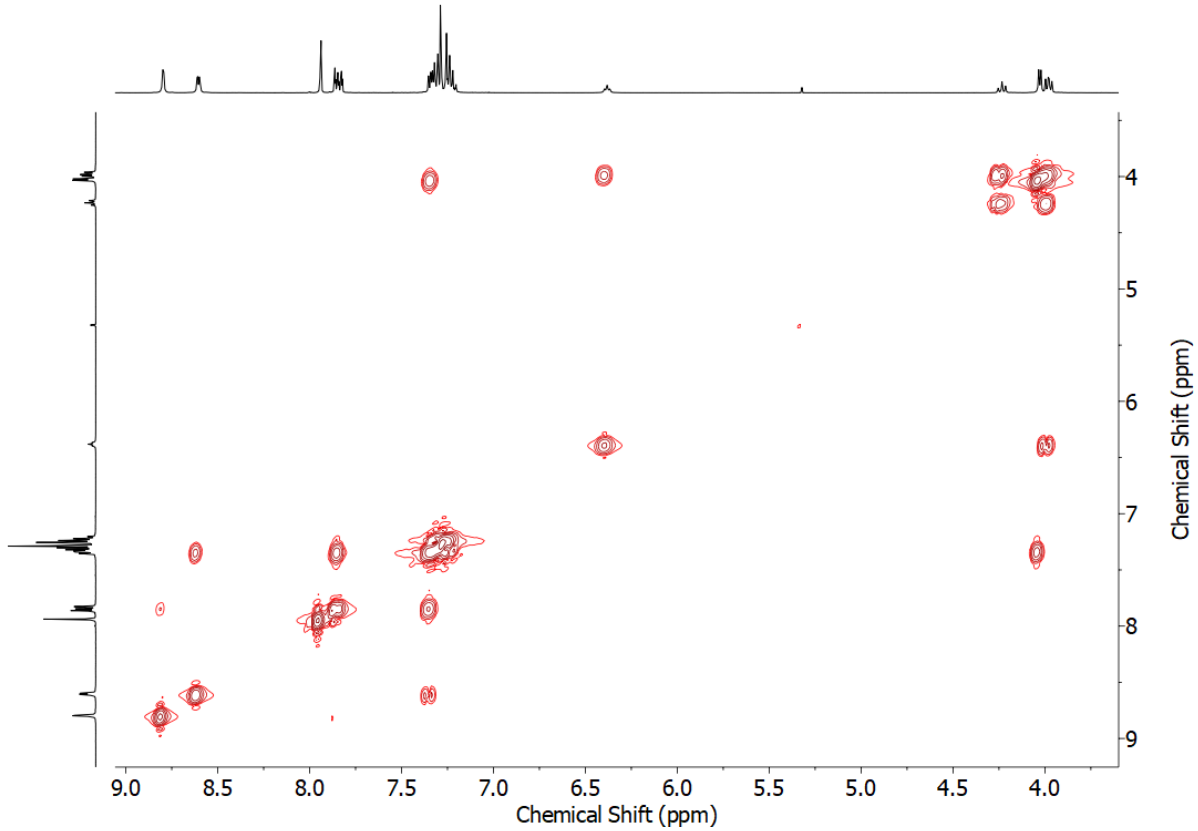

Figure S8 COSY NMR ($CDCl_3$) of **4**.

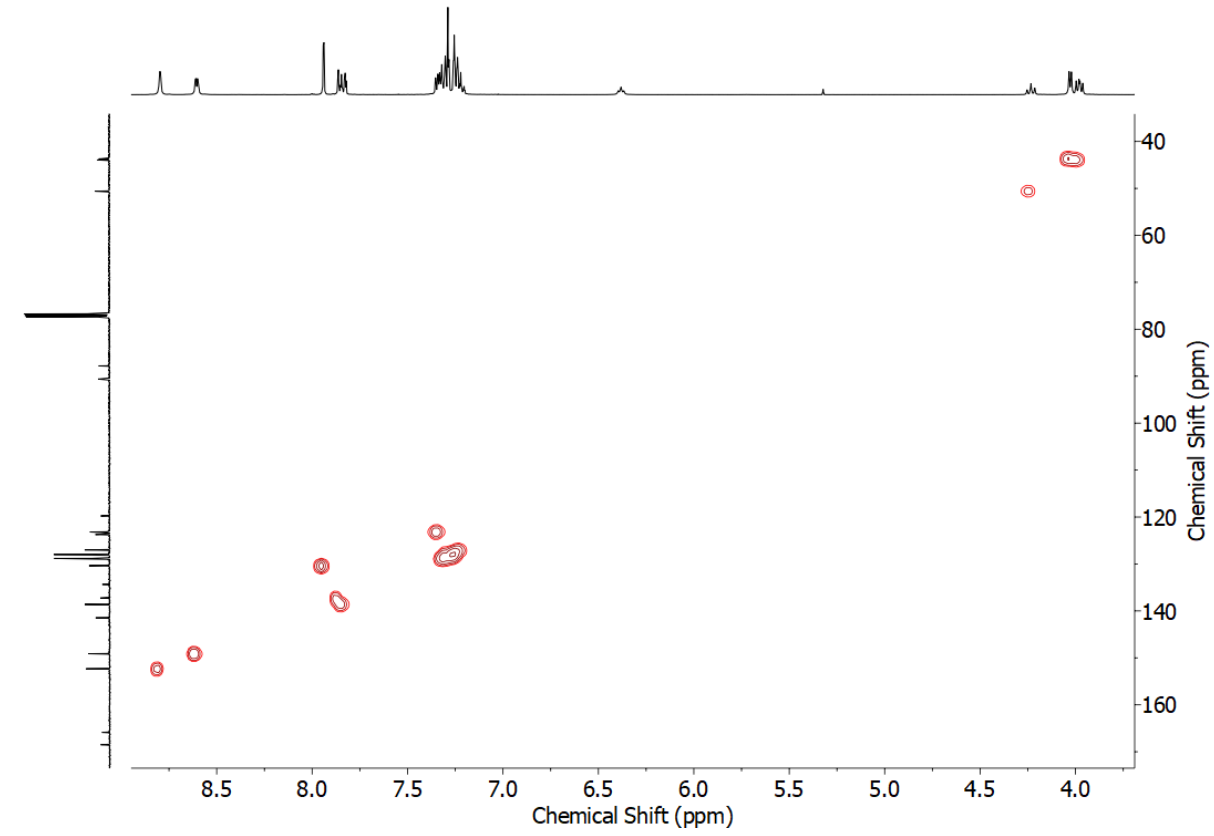

Figure S9 HSQC NMR ($CDCl_3$) of **4**.

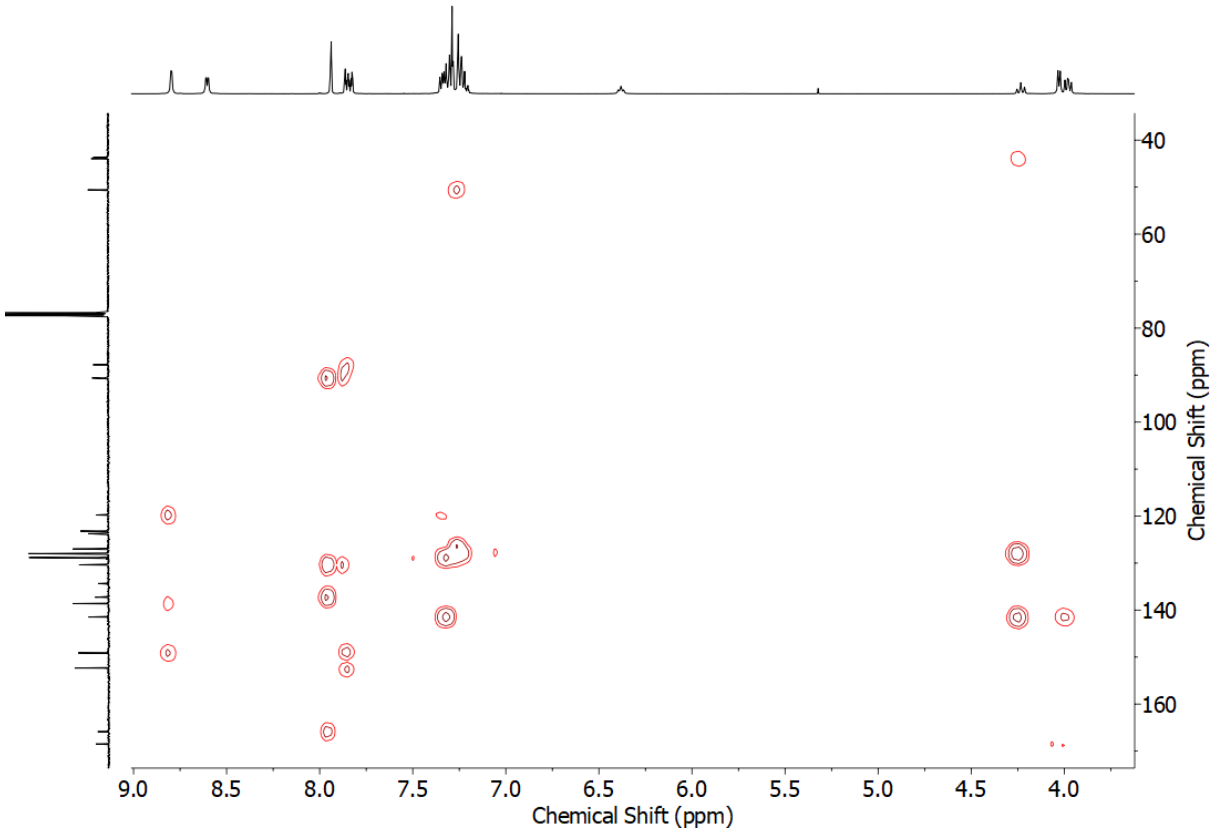

Figure S10 HMBC NMR ($CDCl_3$) of **4**.

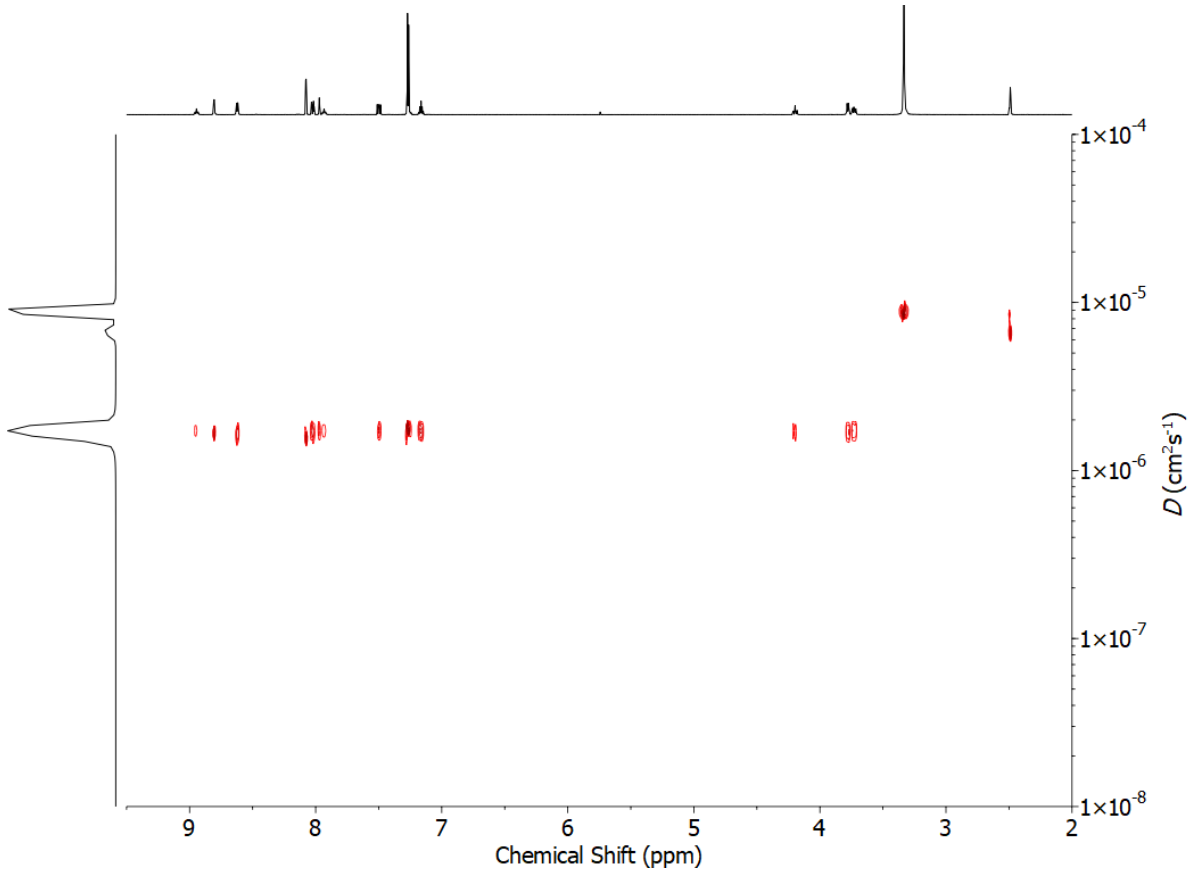

Figure S11 ^{1}H DOSY NMR (d_6-DMSO, 500 MHz) of **4**.

Synthesis of 1

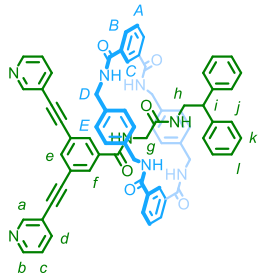

p-Xylylenediamine (0.545 g, 4.0 mmol, 8 eq.) in $CHCl_3$ (25mL) and isophthaloyl dichloride (0.812 g, 4.0 mmol, 8 eq.) in $CHCl_3$ (25mL) were added simultaneously over 4 h to **4** (0.280 g, 0.50 mmol, 1 eq.) and NEt_3 (1.2 mL, 8.0 mmol, 16 eq.) in $CHCl_3$ (75 mL) before stirring at rt overnight. The reaction mixture was washed with 1 M $HCl_{(aq)}$ (3 × 50 mL), sat. aq. $NaHCO_3$ (2 × 100 mL) and brine (2 × 50 mL), dried ($MgSO_4$) and the solvent removed *in vacuo*. After purification by column chromatography (3:7 acetone/CH_2Cl_2) the product was obtained as a white solid (0.053 g, 0.048 mmol, 10%). M.p. 152-154 °C. ^{1}H NMR (400 MHz, $CDCl_3$) δ: 8.67 (s, 2H, H_a), 8.58 (dd, *J* = 4.9, 1.7 Hz, 2H, H_b), 8.40 (s, 2H, H_C), 8.21 (br. s, 1H, H_{NH}), 8.05 (dd, *J* = 7.8, 1.3 Hz, 4H, H_B), 7.84 (t, *J* = 1.4 Hz, 1H, H_e), 7.78 (app. dt, *J* = 7.9, 1.8 Hz, 2H, H_d), 7.58 (t, *J* = 5.0 Hz, 4H, H_{NH}), 7.53 (d, *J* = 1.4 Hz, 2H, H_f), 7.48 (t, *J* = 7.8 Hz, 2H, H_A), 7.31 (dd, *J* = 7.6, 4.9 Hz, 2H, H_c), 7.27-7.15 (m, 10H, H_j, H_k, H_l), 6.94 (s, 8H, H_E), 7.36 (t, *J* = 4.2 Hz, 1H, H_{NH}), 4.46 (d, *J* = 5.1 Hz, 8H, H_D), 4.20 (t, *J* = 8.0 Hz, 1H, H_i), 3.88 (dd, *J* = 8.0, 5.4 Hz, 2H, H_h), 2.64 (d, *J* = 4.1 Hz, 2H, H_g). Diffusion coefficient (500 MHz, d_6-DMSO) *D*: 1.26 × 10^{-10} m^2s^{-1}. ^{13}C NMR (101 MHz, $CDCl_3$) δ: 169.2, 166.7, 165.7, 152.5, 149.3, 141.5, 139.0, 138.1, 137.4, 134.0, 133.2, 131.6, 129.7, 129.4, 129.1, 129.0, 128.0, 127.3, 124.2, 124.1, 123.3, 119.5, 89.9, 88.5, 50.7, 44.8, 44.4, 42.1. HR-ESI-MS m/z = 1115.4246 $[M+Na]^+$ calc. 1115.4221.

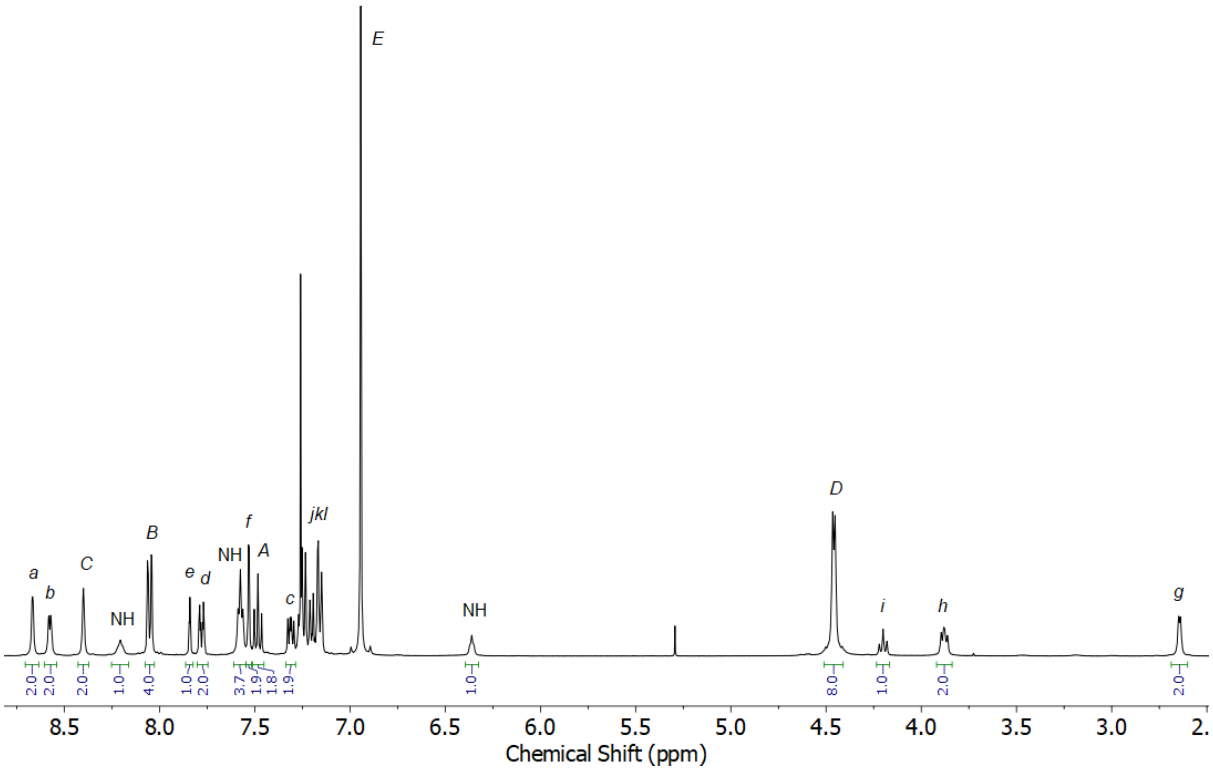

Figure S12 ^{1}H NMR ($CDCl_3$, 400 MHz) of **1**.

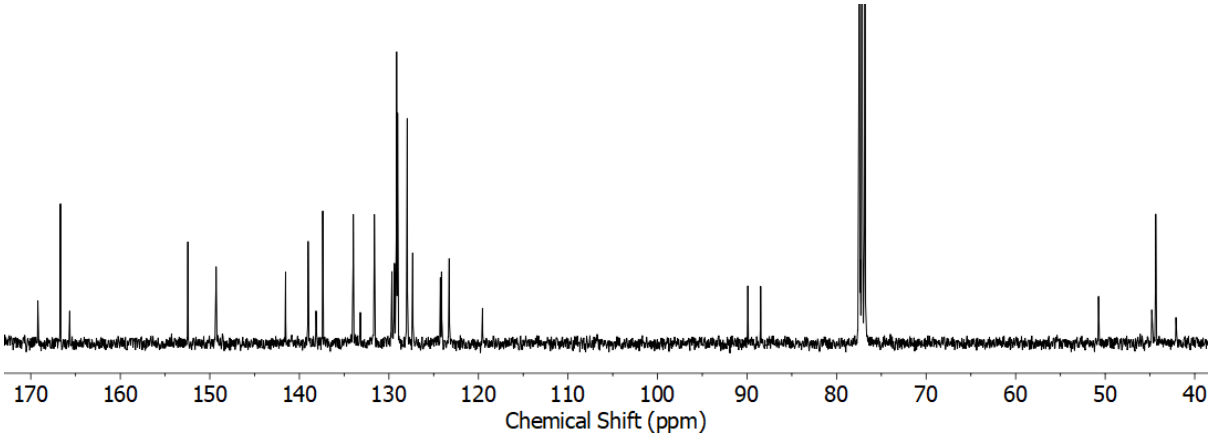

Figure S13 ^{13}C NMR ($CDCl_3$, 101 MHz) of **1**.

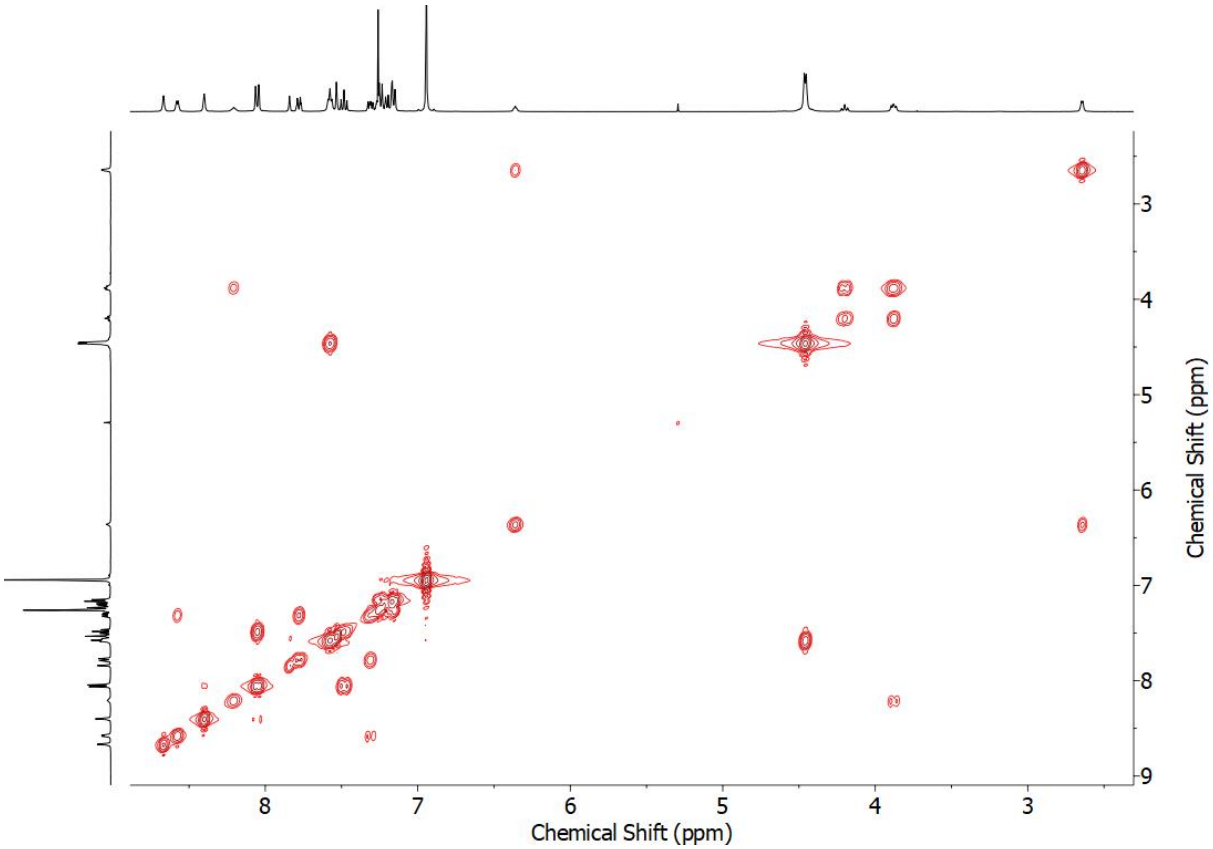

Figure S14 COSY NMR ($CDCl_3$) of **1**.

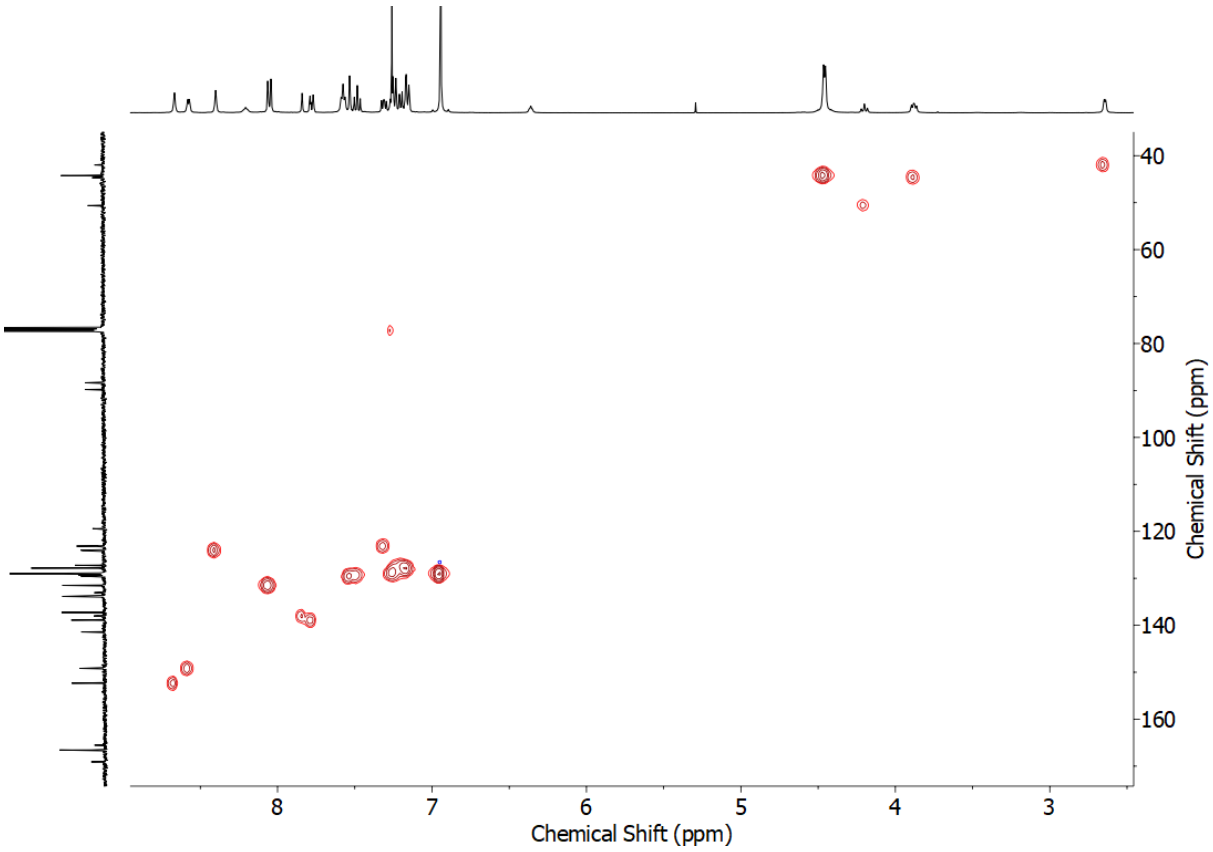

Figure S15 HSQC NMR ($CDCl_3$) of **1**.

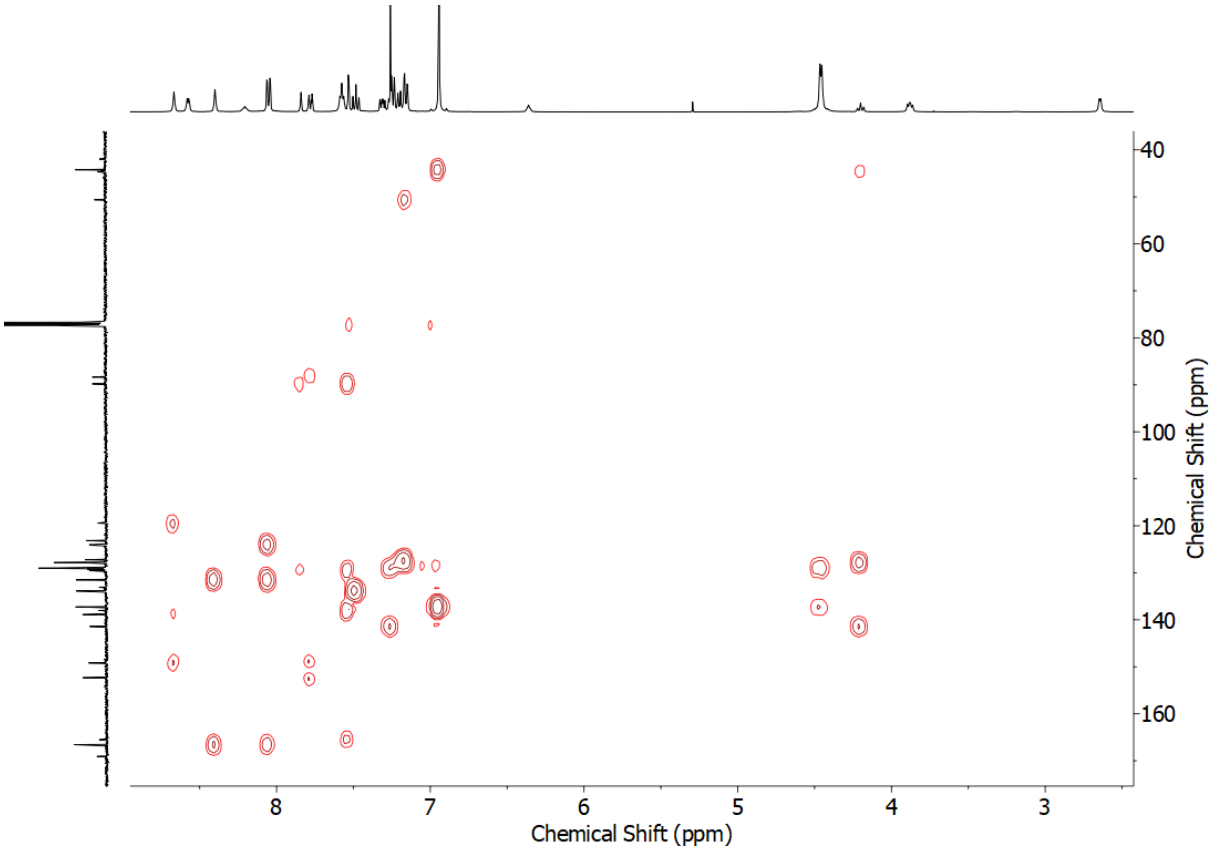

Figure S16 HMBC NMR ($CDCl_3$) of **1**.

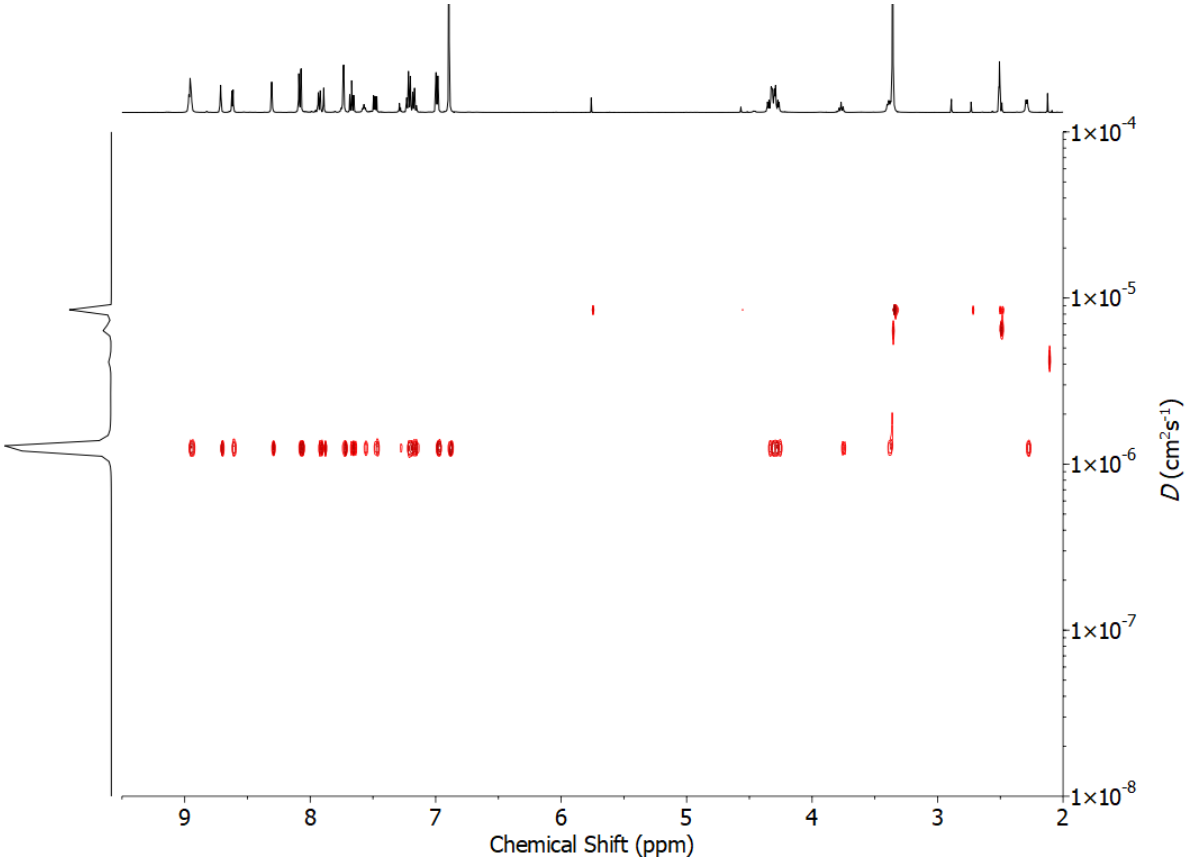

Figure S17 ^{1}H DOSY NMR (d_6-DMSO, 500 MHz) of **1**.

Synthesis of $[Pd_2(4)_4](BF_4)_4$

4 (11.2 mg, 0.020 mmol, 2 eq.) and $[Pd(CH_3CN)_4](BF_4)_2$ (4.4 mg, 0.010 mmol, 1 eq.) were sonicated in d_6-DMSO (0.75 mL) until all solids were dissolved. Quantitative conversion to $[Pd_2(\mathbf{4})_4](BF_4)_4$ was observed by ^{1}H NMR. ^{1}H NMR (400 MHz, d_6-DMSO) δ: 9.64 (d, J = 2.1 Hz, 8H, H_a), 9.39 (m, 8H, H_b), 8.95 (t, J = 5.9 Hz, 4H, H_{NH}), 8.30 (app. dt, J = 7.9, 1.6 Hz, 8H, H_d), 8.17 (d, J = 1.6 Hz, 8H, H_f), 8.07 (t, J = 1.5 Hz, 4H, H_e), 7.96 (t, J = 5.7 Hz, 4H, H_{NH}), 7.84 (dd, J = 8.0, 5.8 Hz, 8H, H_c), 7.28-7.23 (m, 32H, H_j, H_k), 7.17-7.13 (m, 8H, H_l), 4.15 (t, J = 7.7 Hz, 4H, H_i), 3.75 (d, J = 5.6 Hz, 8H, H_g), 3.70 (m, 8H, H_h). Diffusion coefficient (500 MHz, d_6-DMSO) D: 7.76 × 10^{-11} m^2s^{-1}. ^{13}C NMR (101 MHz, d_6-DMSO) δ: 168.5, 164.3, 153.0, 150.8, 142.9, 142.8, 135.9, 135.6, 132.1 (×2), 128.4, 127.9, 127.4, 126.3, 122.0, 93.2, 85.8, 50.0, 43.2, 42.5. ^{19}F (377 MHz, d_6-DMSO) δ: -148.06, -148.12. ESI-MS m/z = 1271.5 calc. $\{[Pd_2(\mathbf{4})_4](HCO_2)_2\}^{2+}$ 1271.3; 832.7 calc. $\{[Pd_2(\mathbf{4})_4](HCO_2)\}^{3+}$ 832.6.

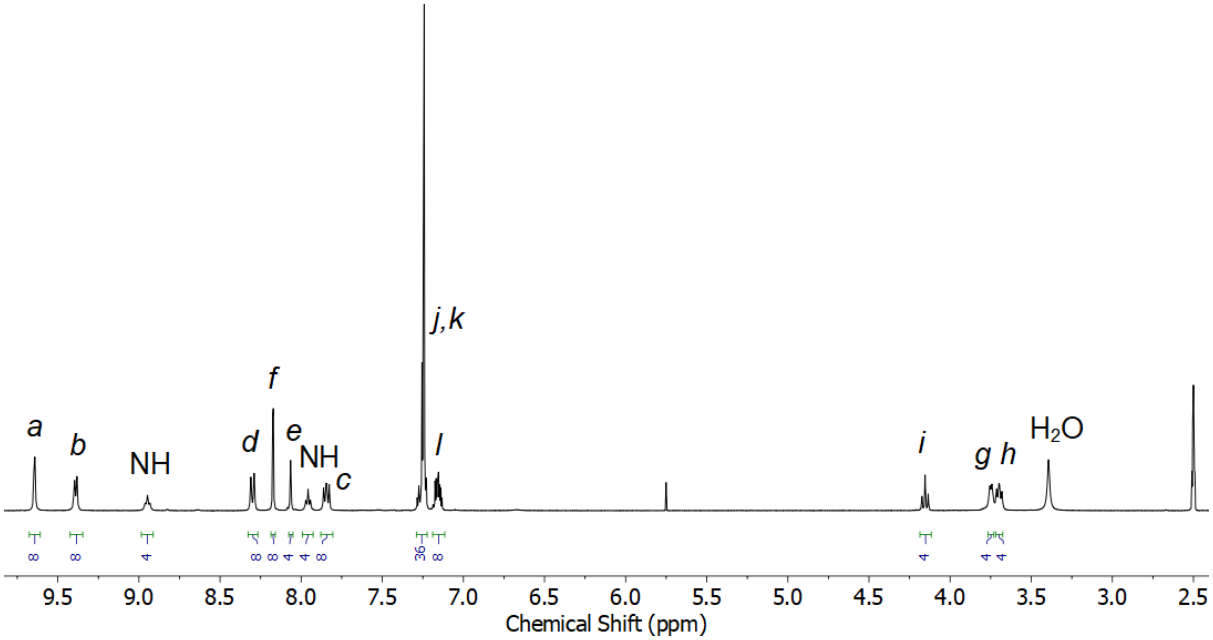

Figure S18 ^{1}H NMR (d_6-DMSO, 400 MHz) of $[Pd_2(\mathbf{4})_4](BF_4)_4$.

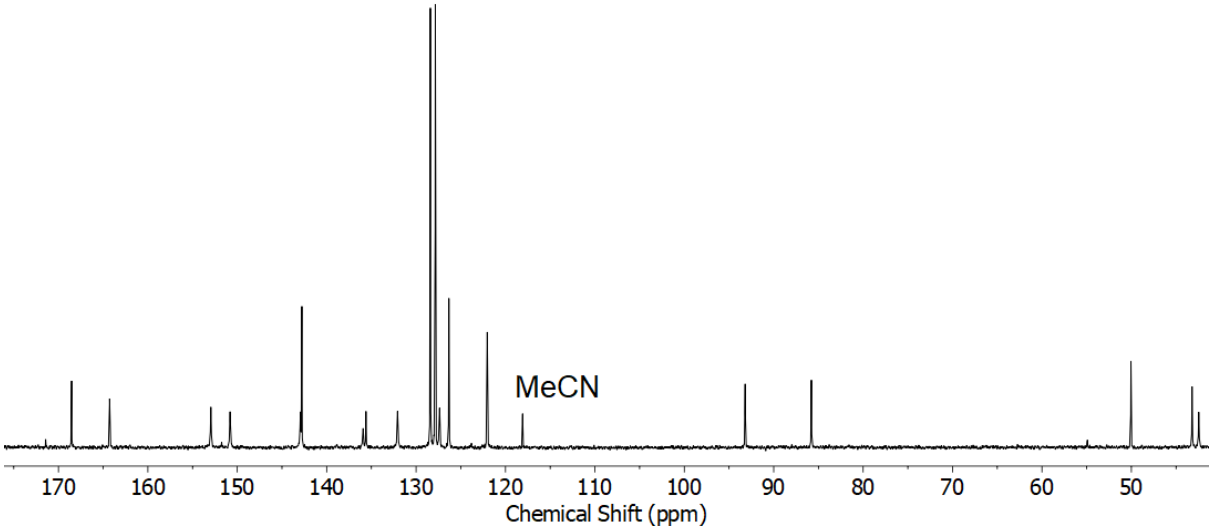

Figure S19 ^{13}C NMR (d_6-DMSO, 101 MHz) of $[Pd_2(\mathbf{4})_4](BF_4)_4$.

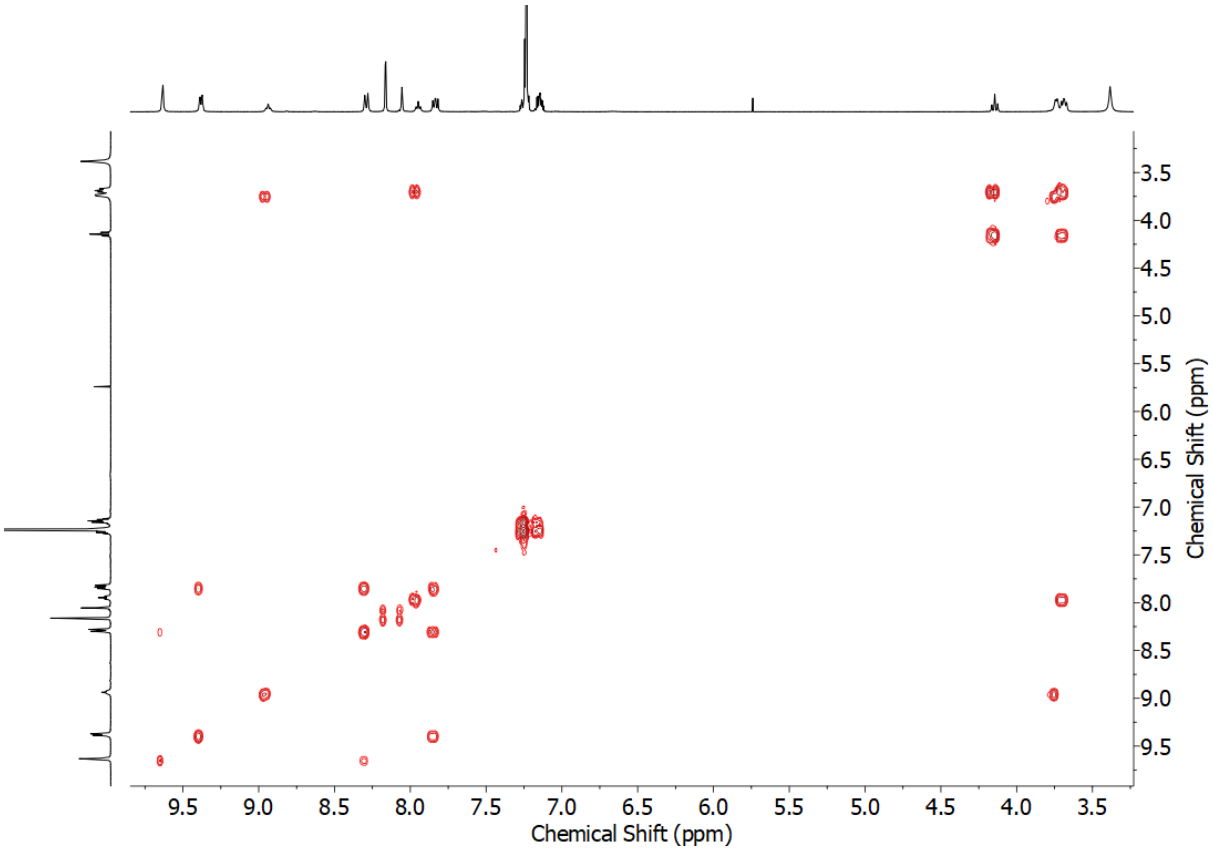

Figure S20 COSY NMR (d_6-DMSO) of $[Pd_2(\mathbf{4})_4](BF_4)_4$.

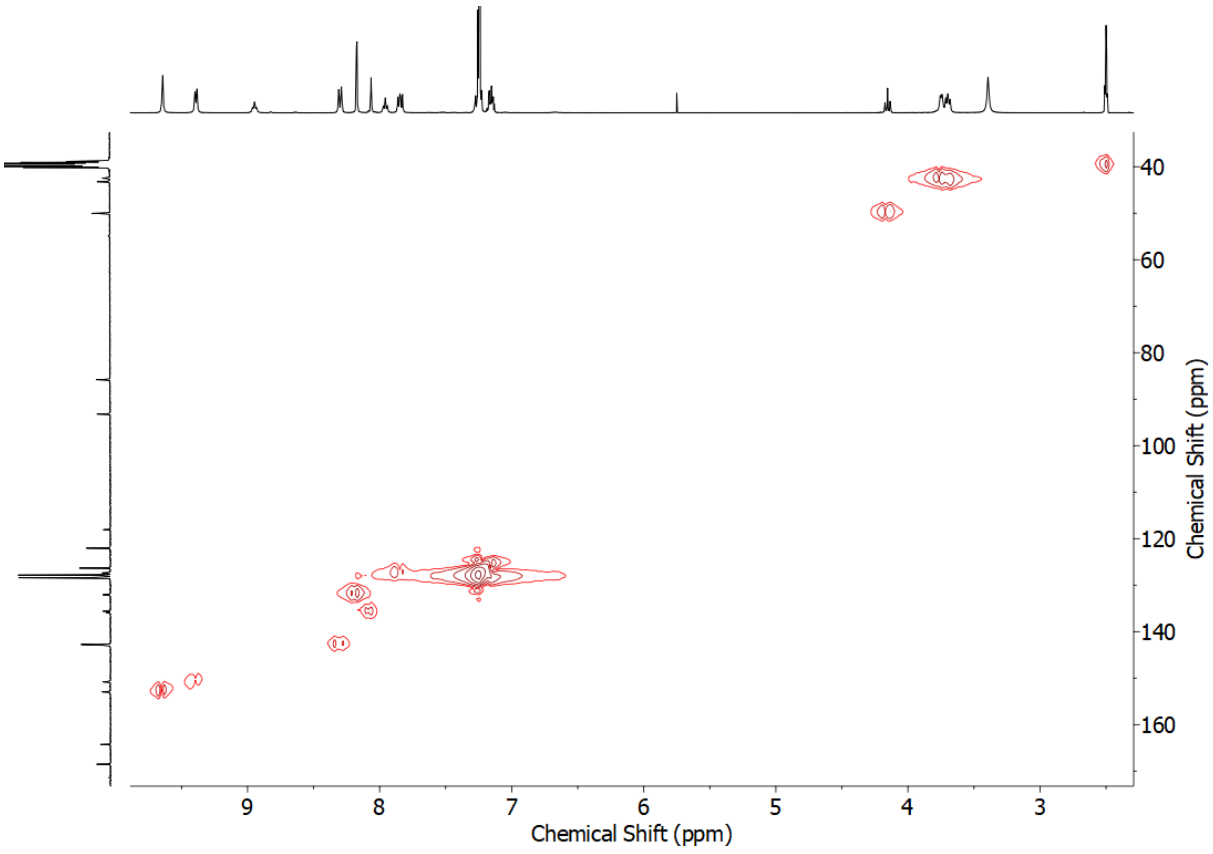

Figure S21 HSQC NMR (d_6-DMSO) of $[Pd_2(\mathbf{4})_4](BF_4)_4$.

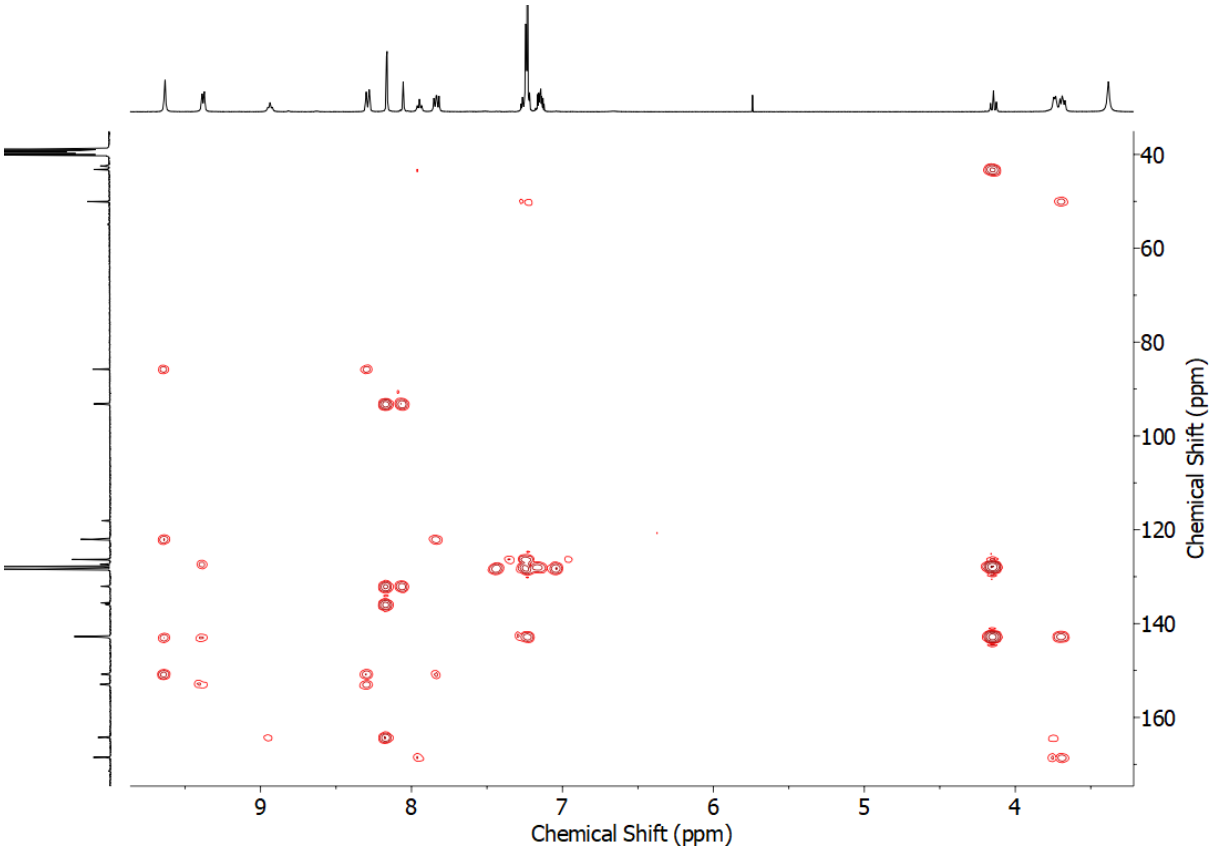

Figure S22 HMBC NMR (d_6-DMSO) of $[Pd_2(\mathbf{4})_4](BF_4)_4$.

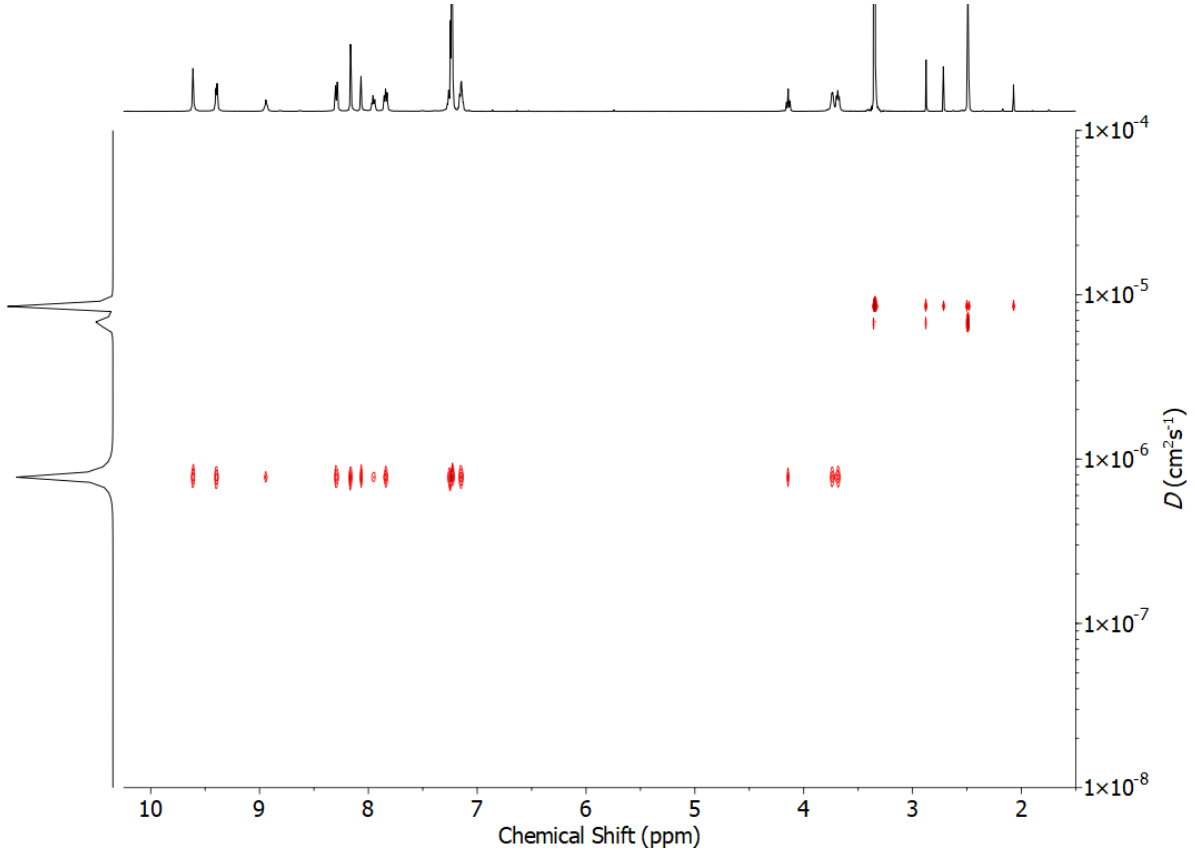

Figure S23 ^{1}H DOSY NMR (d_6-DMSO, 500 MHz) of $[Pd_2(\mathbf{4})_4](BF_4)_4$.

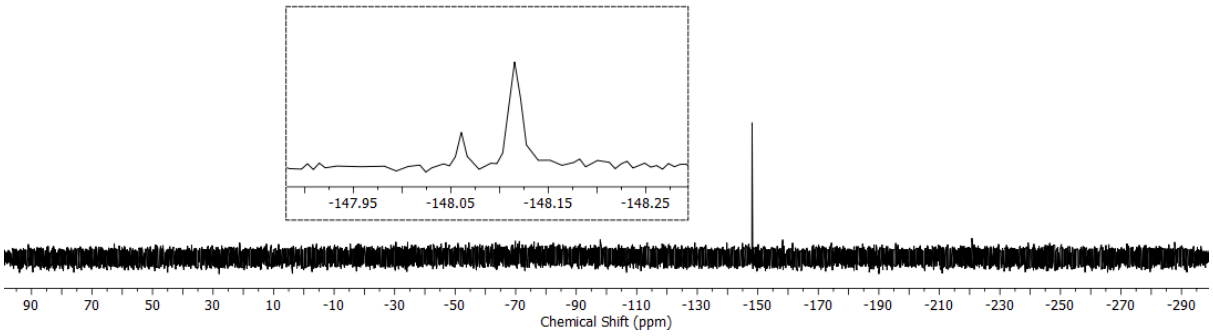

Figure S24 ^{19}F NMR (d_6-DMSO, 377 MHz) of $[Pd_2(\mathbf{4})_4](BF_4)_4$.

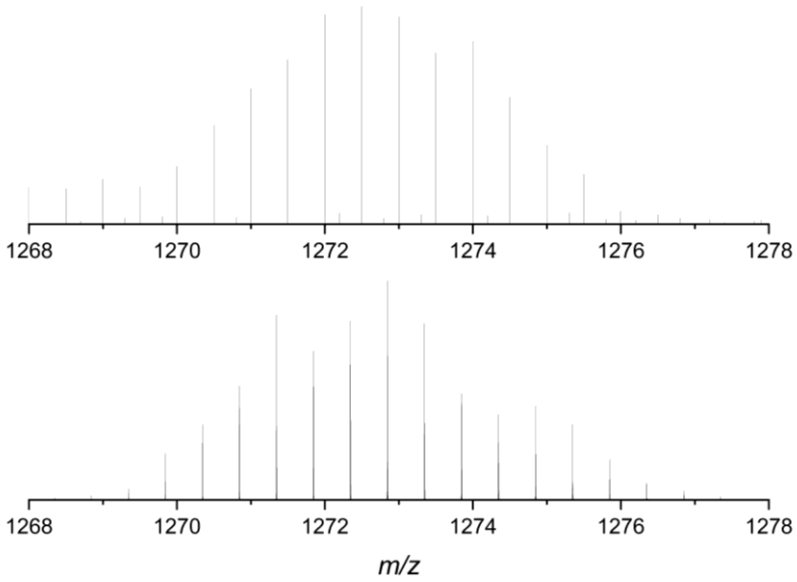

Figure S25 Observed (top) and calculated (bottom) isotopic patterns for $\{[Pd_2(\mathbf{4})_4](HCO_2)_2\}^{2+}$.

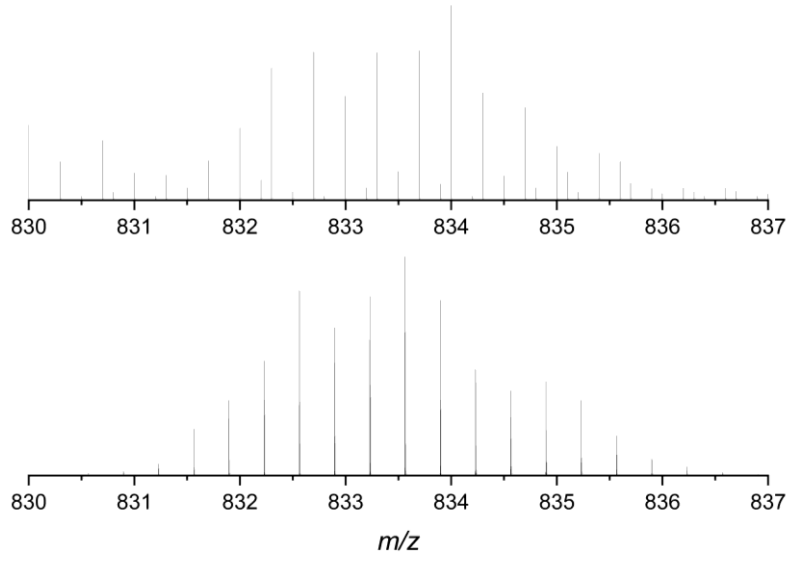

Figure S26 Observed (top) and calculated (bottom) isotopic patterns for $\{[Pd_2(\mathbf{4})_4](HCO_2)\}^{3+}$.

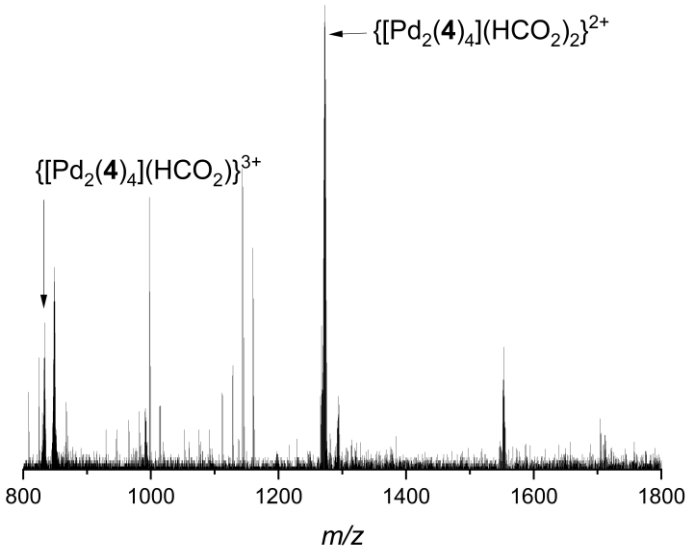

Figure S27 ESI-MS of $[Pd_2(\mathbf{4})_4](BF_4)_4$.

Synthesis of $[Pd_2(1)_4](BF_4)_4$

1 (11.2 mg, 0.020 mmol, 2 eq.) and $[Pd(CH_3CN)_4](BF_4)_2$ (4.4 mg, 0.010 mmol, 1 eq.) were sonicated in d_6-DMSO (0.75 mL) until all solids were dissolved. Quantitative conversion to $[Pd_2(\mathbf{S1})_4](BF_4)_4$ was observed by ^{1}H NMR. ^{1}H NMR (400 MHz, d_6-DMSO) δ: 9.50 (br. s, 8H, H_a), 9.35 (d, J = 6.0 Hz, 8H, H_b), 8.88 (br. m, 16H, H_{NH}), 8.18 (br. s, 8H, H_C), 8.00 (d, J = 7.7 Hz, 16H, H_B), 7.95 (d, J = 8.0 Hz, 8H, H_d), 7.90 (s, 4H, H_e), 7.82-7.79 (m, 8H, H_c), 7.74 (s, 8H, H_f), 7.68 (br. m, 4H, H_{NH}), 7.62 (app. t, J = 7.7 Hz, 12H, H_A, H_{NH}), 7.18-7.11 (m, 24H, 2 of $H_{j/k/l}$), 6.98-6.96 (m, 16H, 1 of $H_{j/k/l}$), 6.77 (s, 32H, H_E), 4.18 (br. m, 32H, H_D), 3.75 (t, J = 8.1 Hz, 4H, H_i), 3.38 (from HSQC, 8H, H_h), 2.14 (br. m, 8H, H_g). Diffusion coefficient (500 MHz, d_6-DMSO) D: 6.87 × 10^{-11} m^2s^{-1}. ^{13}C NMR (101 MHz, d_6-DMSO) δ: 171.6, 167.9, 166.3, 164.8, 152.8, 150.8, 142.7, 142.5, 137.1, 135.5, 134.5, 131.8, 130.1, 128.7, 128.4, 128.3, 127.9, 127.5, 127.3, 126.4, 122.0, 121.8, 92.9, 85.7, 50.2, 43.8, 43.0, 39.7 (HSQC). ^{19}F (377 MHz, d_6-DMSO) δ: -148.01, -148.07. ESI-MS m/z = 1542.2 calc. $\{[Pd_2(\mathbf{1})_4](HCO_2)\}^{3+}$ 1542.2; 1145.4 calc. $\{[Pd_2(\mathbf{1})_4]\}^{4+}$ 1145.4

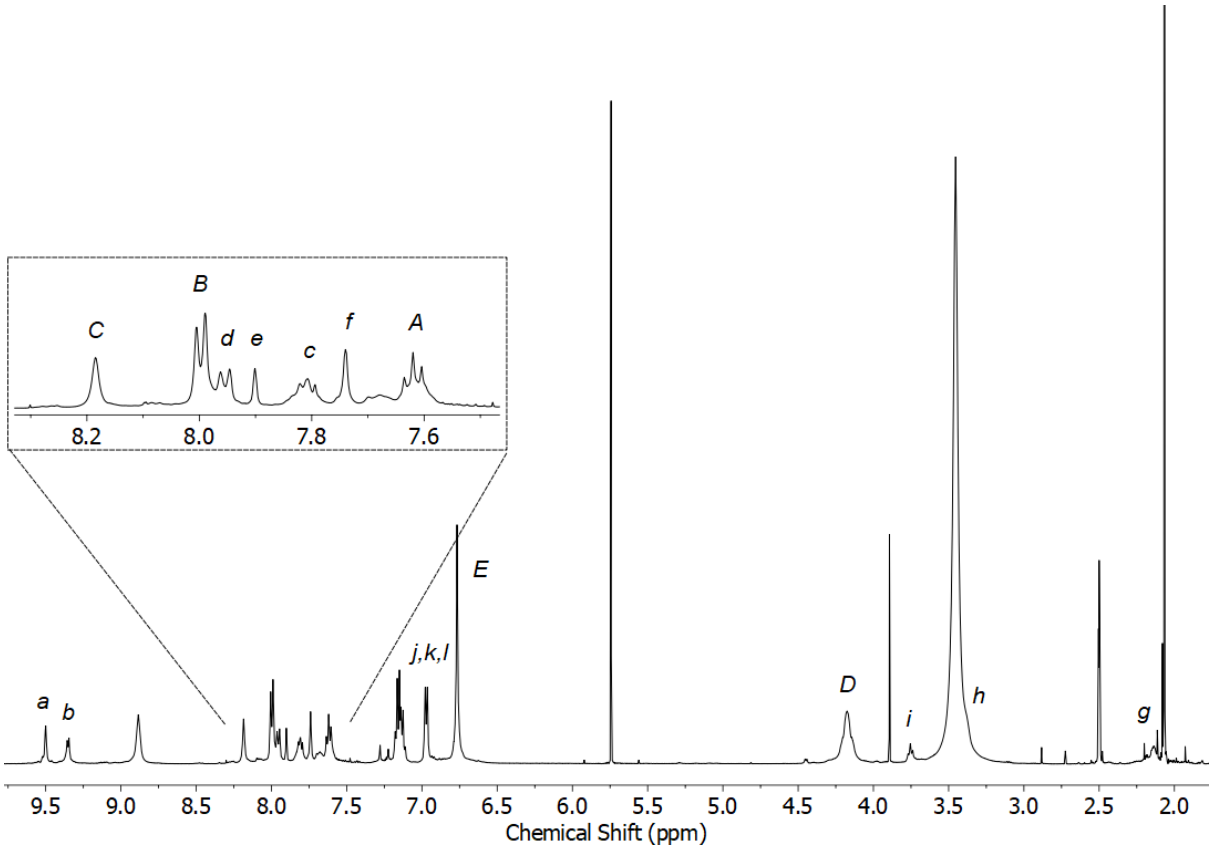

Figure S28 ^{1}H NMR (d_6-DMSO, 500 MHz) of $[Pd_2(\mathbf{1})_4](BF_4)_4$.

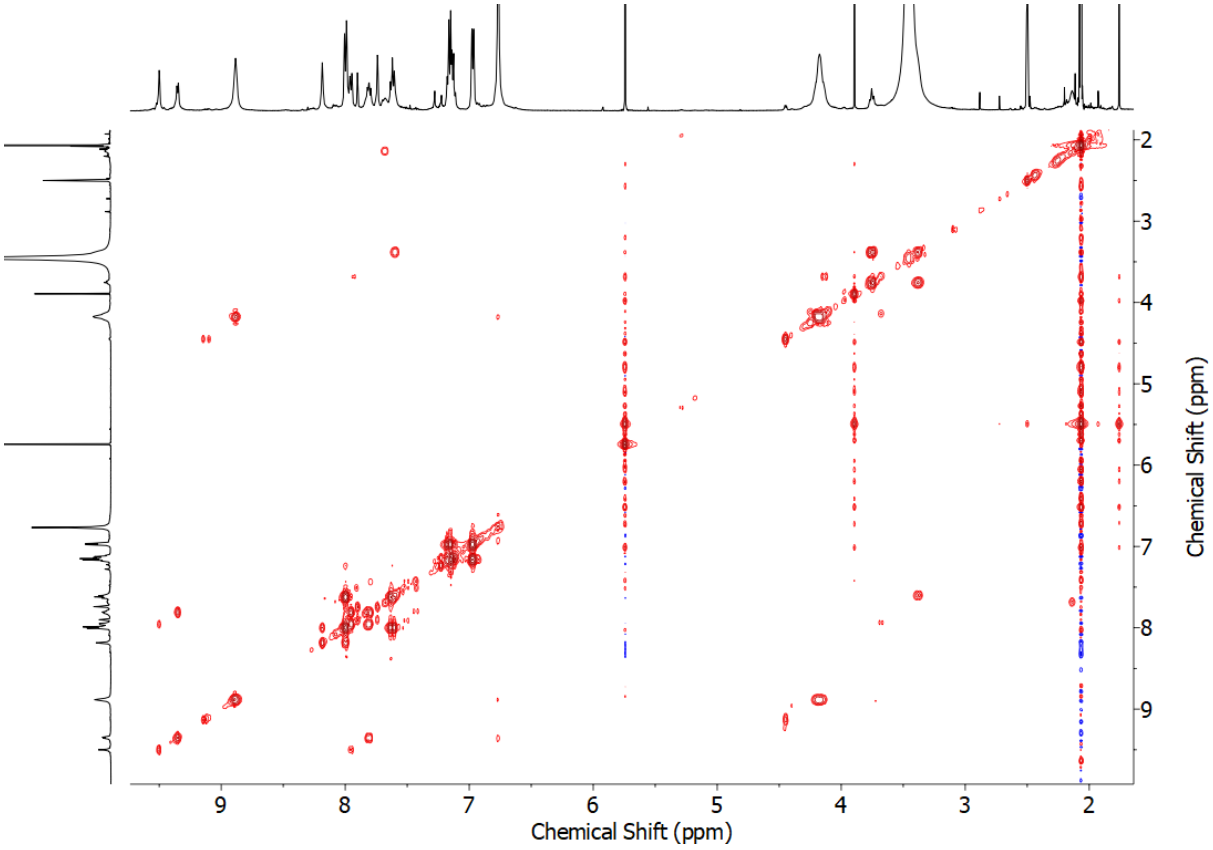

Figure S29 COSY NMR (d_6-DMSO) of $[Pd_2(\mathbf{1})_4](BF_4)_4$.

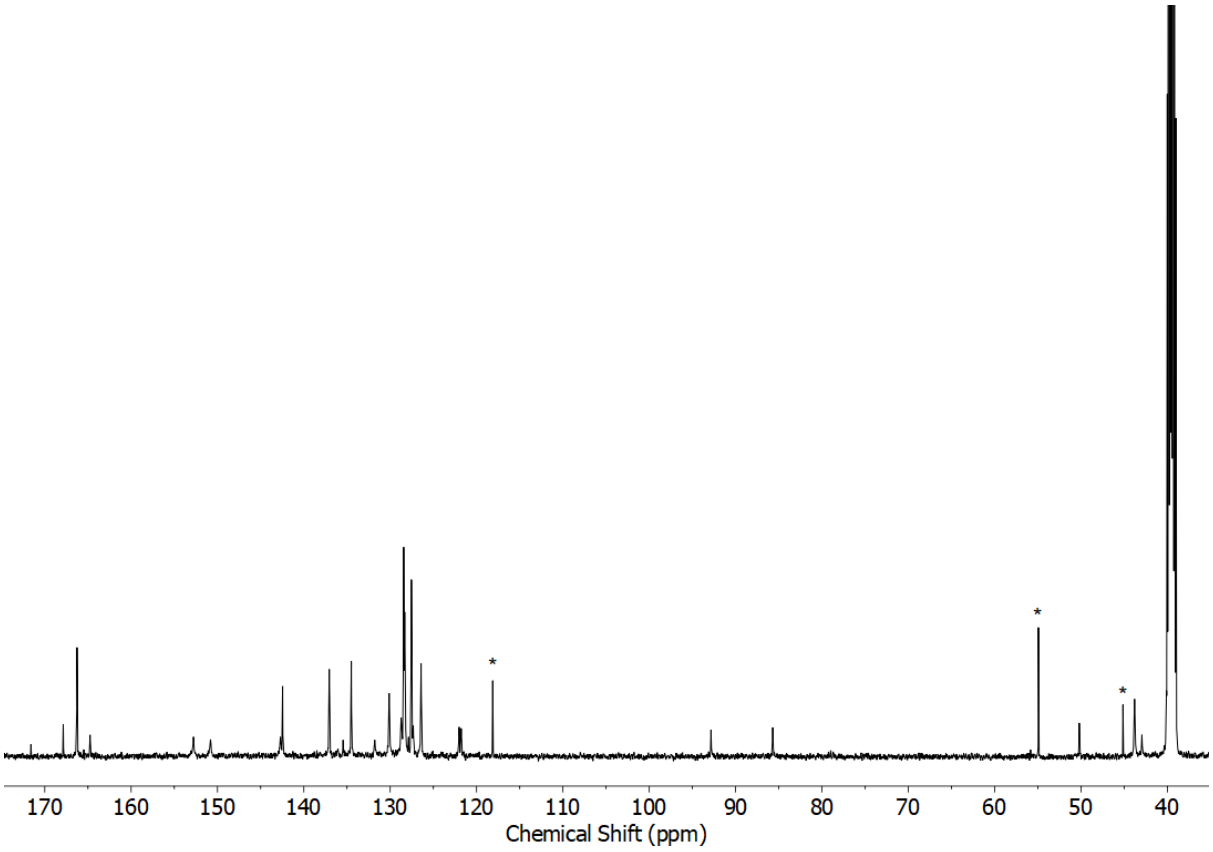

Figure S30 ^{13}C NMR (d_6-DMSO, 126 MHz) of $[Pd_2(\mathbf{1})_4](BF_4)_4$.

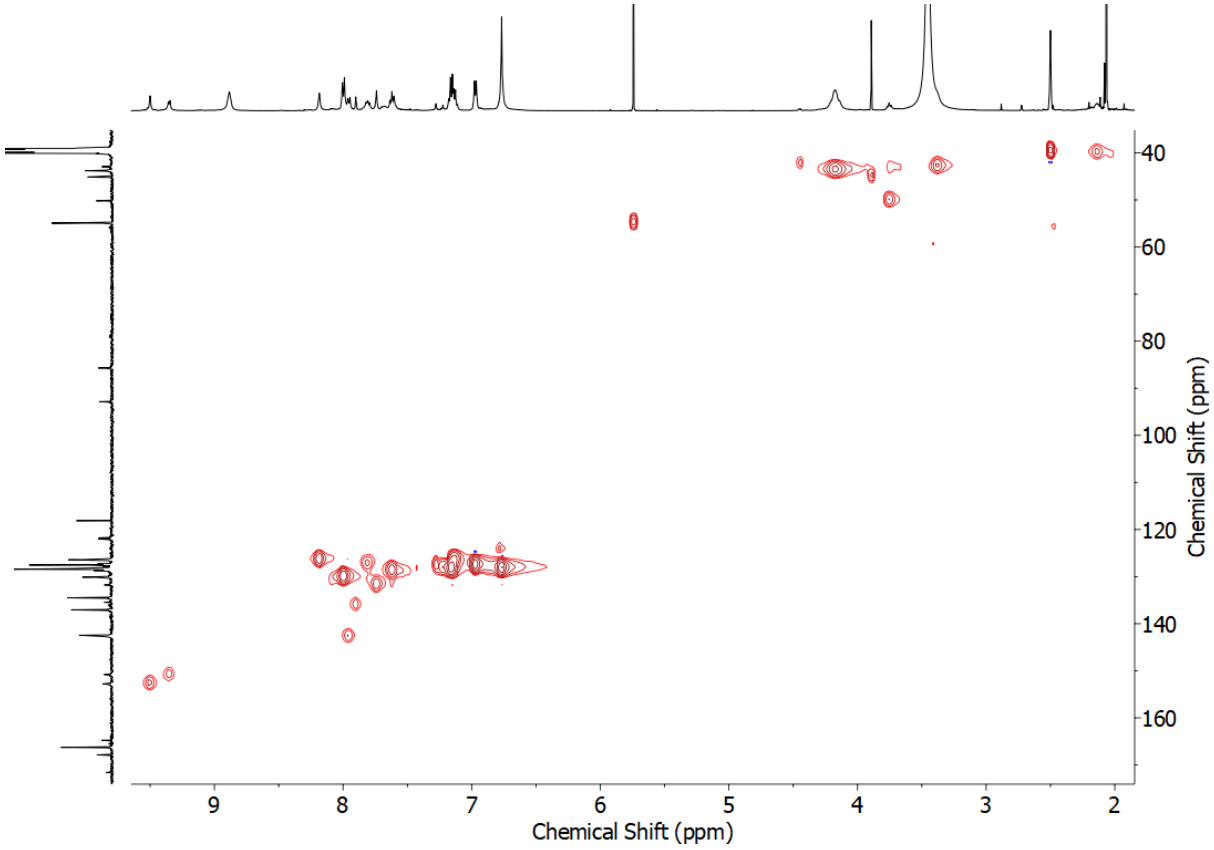

Figure S31 HSQC NMR (d_6-DMSO) of $[Pd_2(\mathbf{1})_4](BF_4)_4$.

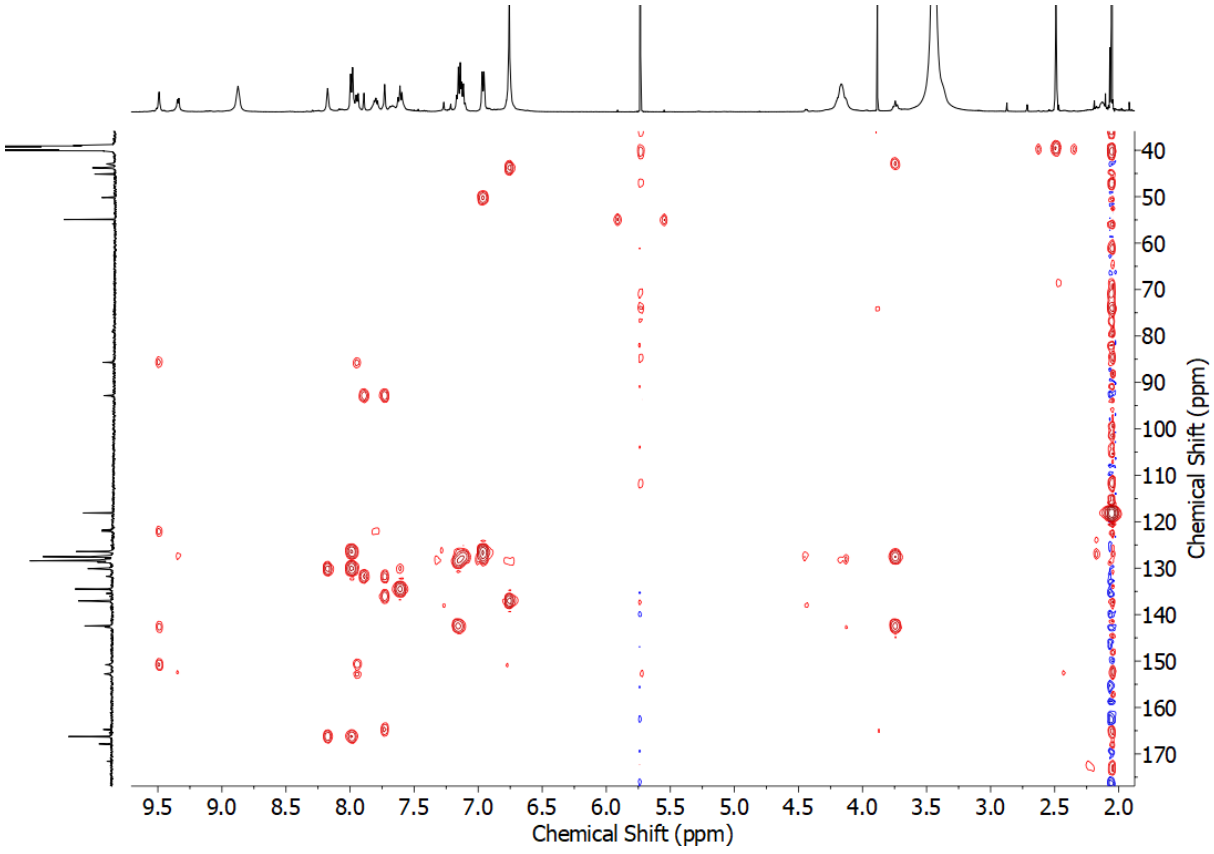

Figure S32 HMBC NMR (d_6-DMSO) of $[Pd_2(\mathbf{1})_4](BF_4)_4$.

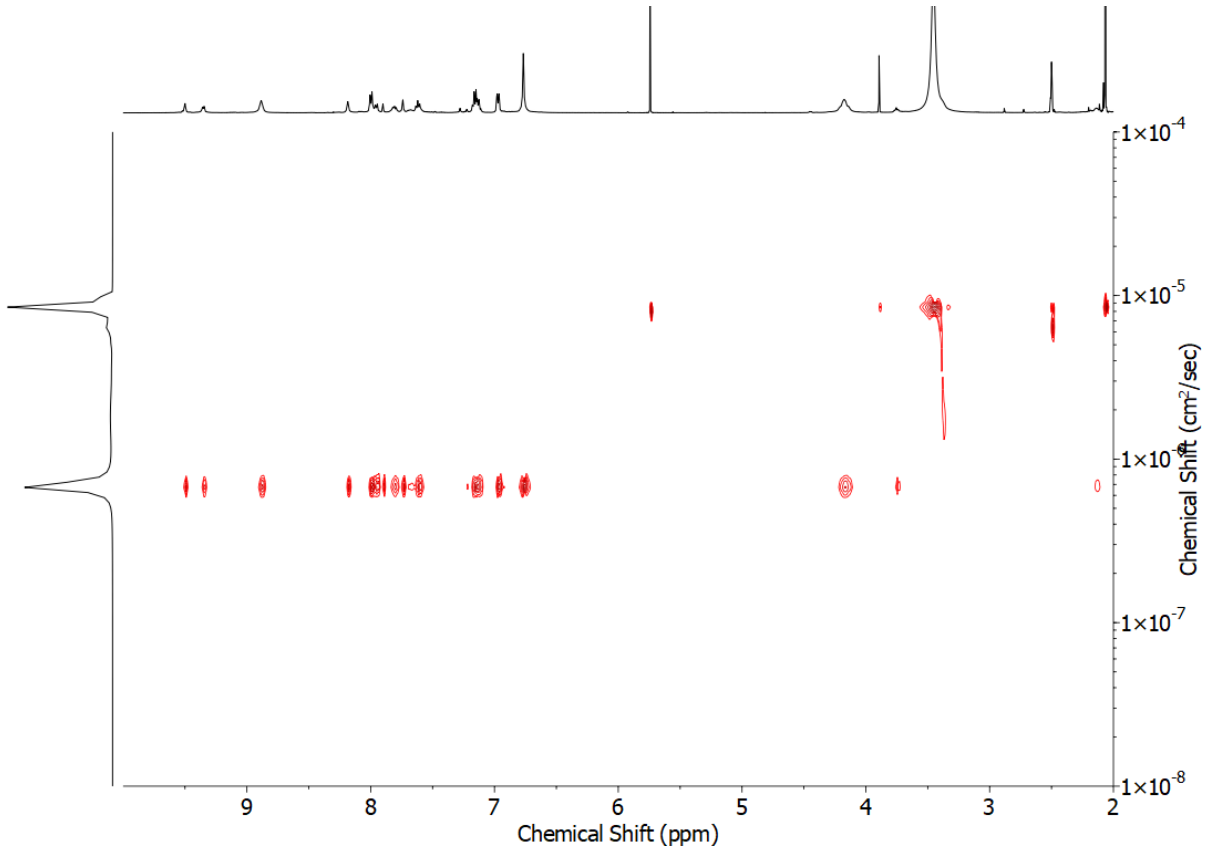

Figure S33 ^{1}H DOSY NMR (d_6-DMSO, 500 MHz) of $[Pd_2(\mathbf{1})_4](BF_4)_4$.

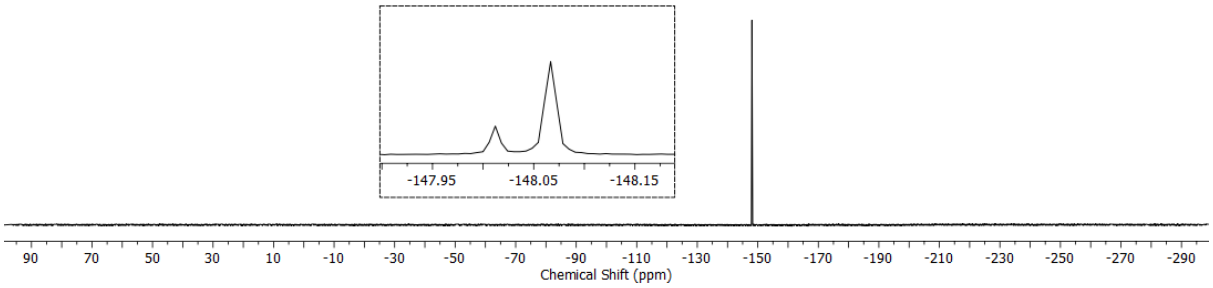

Figure S34^{19}F NMR (d_6-DMSO, 377 MHz) of $[Pd_2(\mathbf{1})_4](BF_4)_4$.

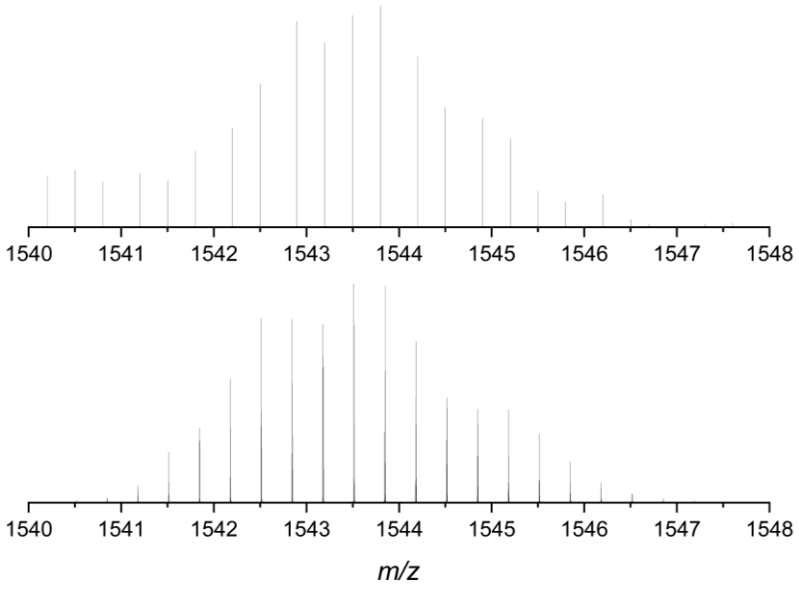

Figure S35 Observed (top) and calculated (bottom) isotopic patterns for $\{[Pd_2(\mathbf{1})_4](HCO_2)\}^{3+}$.

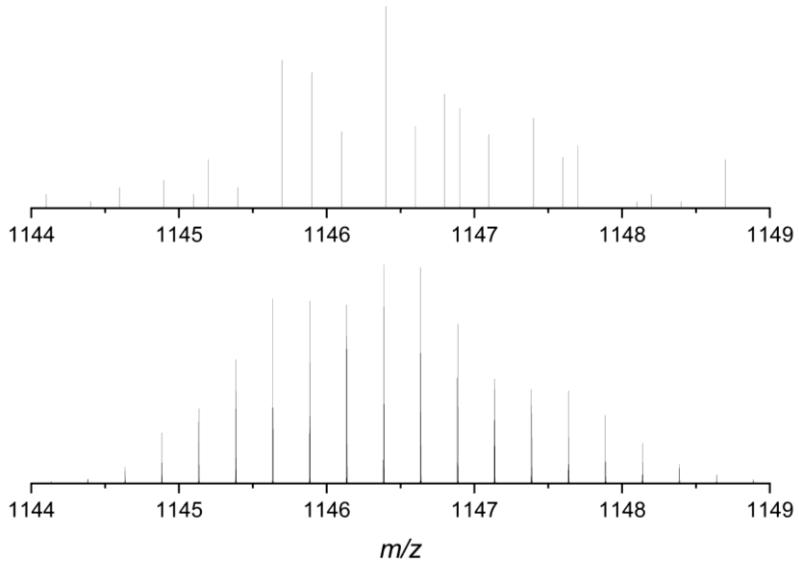

Figure S36 Observed (top) and calculated (bottom) isotopic patterns for $\{[Pd_2(\mathbf{1})_4]\}^{4+}$.

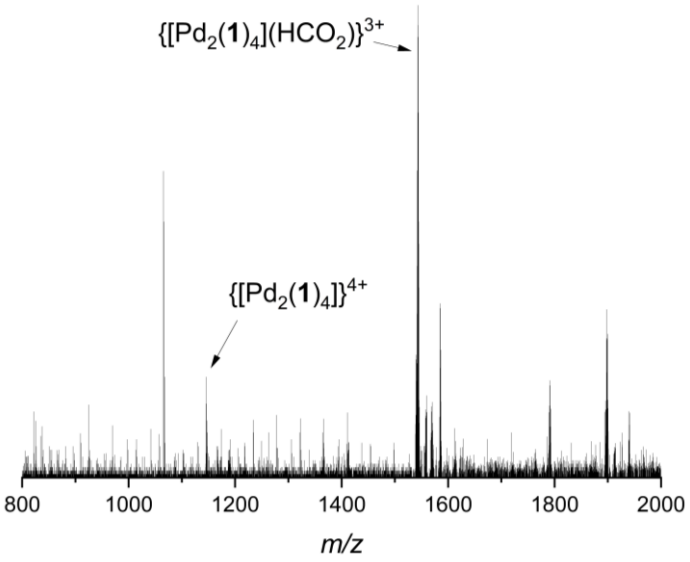

Figure S37 ESI-MS of $[Pd_2(\mathbf{1})_4](BF_4)_4$.

Geometry Optimised Structures

Molecular mechanics models were constructed using Avogadro[2] starting from crystal structures for the $[Pd_2(\mathbf{L})_4]^{4+}$ core (**L** = 1,3-bis(pyridin-3-ylethynyl)benzene; CCDC 768969) and [2]rotaxane **1** (CCDC 2001103) for the axle/rotaxane components and energy-minimised using UFF.[3] Geometry optimisations were subsequently performed using the semi-empirical method PM6[4] in Gaussian 16.[5]

$[Pd_2(4)_4]^{4+}$ Optimised Structure

Overview Tab Data Section:
Calculation Type = FOPT
Calculation Method = RPM6
Formula = $C_{148}H_{112}N_{16}O_8Pd_2$
Basis Set = ZDO
Charge = 4
Spin = Singlet
Solvation = None
E(RPM6) = 2.1335773 Hartree
RMS Gradient Norm = 1.934e-06 Hartree/Bohr
Dipole Moment = 18.842415 Debye
Point Group = C1
Molecular Mass = 2452.6919 amu

Opt Tab Data Section:
Step number = 62
Maximum force = 1e-05 Converged
RMS force = 1e-06 Converged
Maximum displacement = 0.001705 Converged
RMS displacement = 0.000237 Converged
Predicted energy change = -5.275056e-09 Hartree

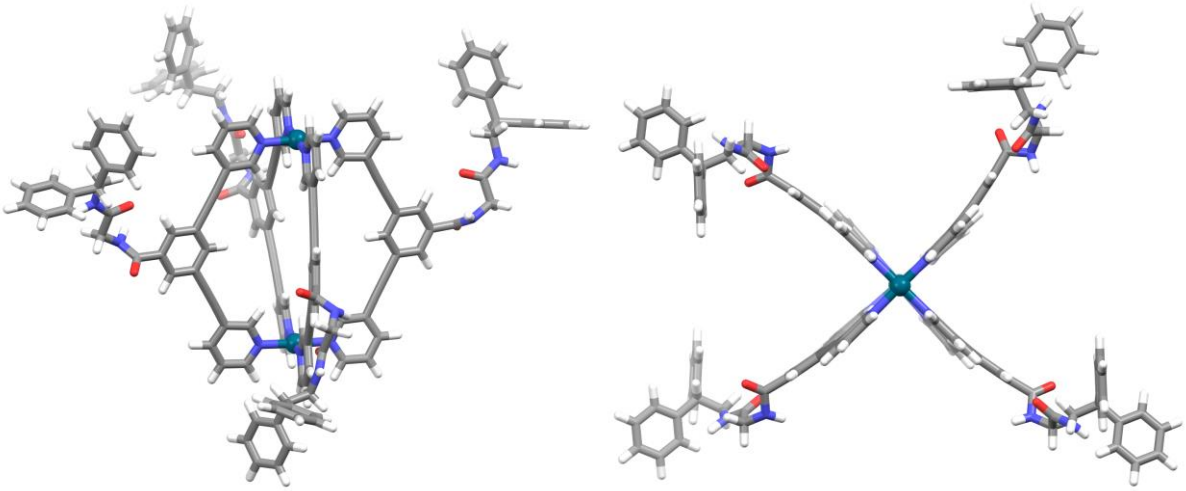

Figure S38 Geometry optimised structure (PM6) of $[Pd_2(\mathbf{4})_4]^{4+}$ shown from the side (left) and down the Pd-Pd axis (right).

$[Pd_2(1)_4]^{4+}$ Optimised Structure

Overview Tab Data Section:
Calculation Type = FOPT
Calculation Method = RPM6
Formula = $C_{276}H_{224}N_{32}O_{24}Pd_2$
Basis Set = ZDO
Charge = 4
Spin = Singlet
Solvation = None
E(RPM6) = 1.4554022 Hartree
RMS Gradient Norm = 1.981e-06 Hartree/Bohr
Dipole Moment = 24.324538 Debye
Point Group = C1
Molecular Mass = 4581.5361 amu

Opt Tab Data Section:
Step number = 226
Maximum force = 4e-05 Converged
RMS force = 3e-06 Converged
Maximum displacement = 0.001134 Converged
RMS displacement = 0.000133 Converged
Predicted energy change = -1.155544e-08 Hartree

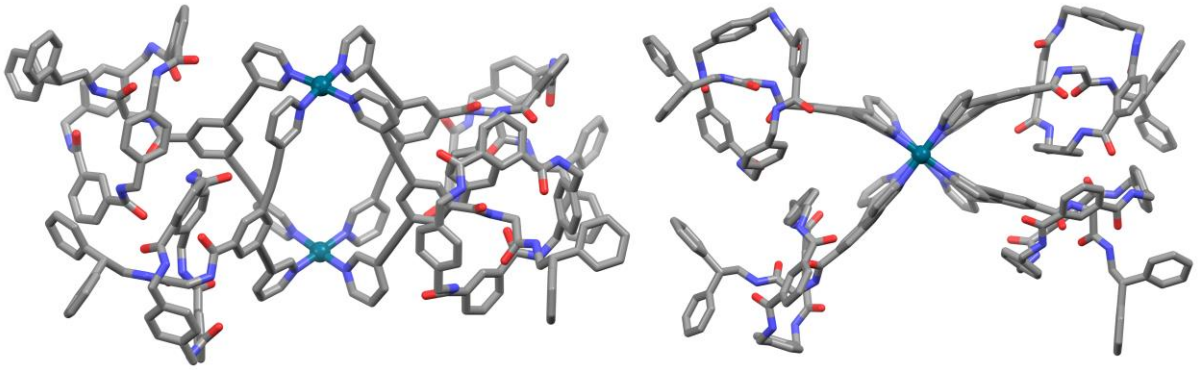

Figure S39 Geometry optimised structure (PM6) of $[Pd_2(\mathbf{1})_4]^{4+}$ shown from the side (left) and down the Pd-Pd axis (right). Hydrogen atoms have been omitted for clarity.

Hydrodynamic Radii Calculations

Hydrodynamic radii were calculated using a variation of the Stokes-Einstein equation:

$$R_H = \frac{k_B T}{6\pi\eta D}$$

Where R_H is the hydrodynamic radius (m)

k_B is the Boltzmann constant (1.38×10^{-23} J K^{-1})

T is the temperature (K)

η is the solvent viscosity (2.180×10^{-3} kg $s^{-1}m^{-1}$ for d_6-DMSO)[6]

D is the diffusion coefficient (m^2s^{-1})

X-ray Crystallography

X-ray quality crystals of [2]rotaxane **1** were grown by vapour diffusion of cyclohexane into a solution of the compound in 1,2-dichloroethane.

Crystal data for **1**: $(C_{37}H_{28}N_4O_2)(C_{32}H_{28}N_4O_4)\cdot 3.5(C_2H_4Cl_2)$, M = 1439.55, monoclinic, $P2_1/c$ (no. 14), a = 23.7142(10), b = 24.8126(5), c = 26.7983(10) Å, β = 108.122(4)°, V = 14986.2(10) Å^3, Z = 8 [2 independent complexes], D_c = 1.276 g cm^{-3}, μ(Mo-Kα) = 0.321 mm^{-1}, T = 173 K, colourless blocks, Agilent Xcalibur 3 E diffractometer; 30190 independent measured reflections (R_{int} = 0.0354), F^2 refinement,[7][8] R_1(obs) = 0.0728, wR_2(all) = 0.2263, 13679 independent observed absorption-corrected reflections [$|F_o| > 4\sigma(|F_o|)$, completeness to θ_{full}(25.2°) = 99.0%], 1544 parameters. CCDC 2001103.

The structure of **1** was found to crystallise with two independent [2]rotaxanes (**1-A** and **1-B**) in the asymmetric unit. The C28-based pyridyl ring in rotaxane **1-A** was found to be disordered. Two orientations were identified of *ca*. 86 and 14% occupancy, their geometries were optimised, the thermal parameters of adjacent atoms were restrained to be similar, and only the non-hydrogen atoms of the major occupancy orientation were refined anisotropically (those of the minor occupancy orientation were refined isotropically).

The included solvent was found to be highly disordered, and the best approach to handling this diffuse electron density was found to be the SQUEEZE routine of PLATON.[9] This suggested a total of 1352 electrons per unit cell, equivalent to 169 electrons per [2]rotaxane. Before the use of SQUEEZE the solvent most resembled 1,2-dichloroethane ($C_2H_4Cl_2$, 50 electrons), and 3.5 1,2-dichloroethane molecules corresponds to 175 electrons, so this was used as the solvent present. As a result, the atom list for the asymmetric unit is low by 2 x 3.5($C_2H_4Cl_2$) = $C_{14}H_{28}Cl_{14}$ (and that for the unit cell low by $C_{56}H_{112}Cl_{56}$) compared to what is actually presumed to be present.

The twelve N–H hydrogen atoms (six for each independent [2]rotaxane) were all located from ΔF maps and refined freely subject to an N–H distance constraint of 0.90 Å.

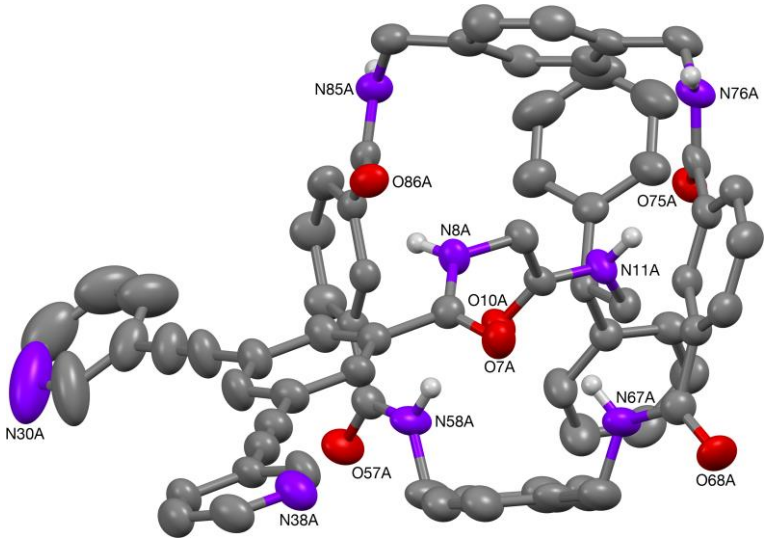

Figure S40 The structure of one (**1-A**) of the two independent [2]rotaxanes present in the crystal of **1** (50% probability ellipsoids).

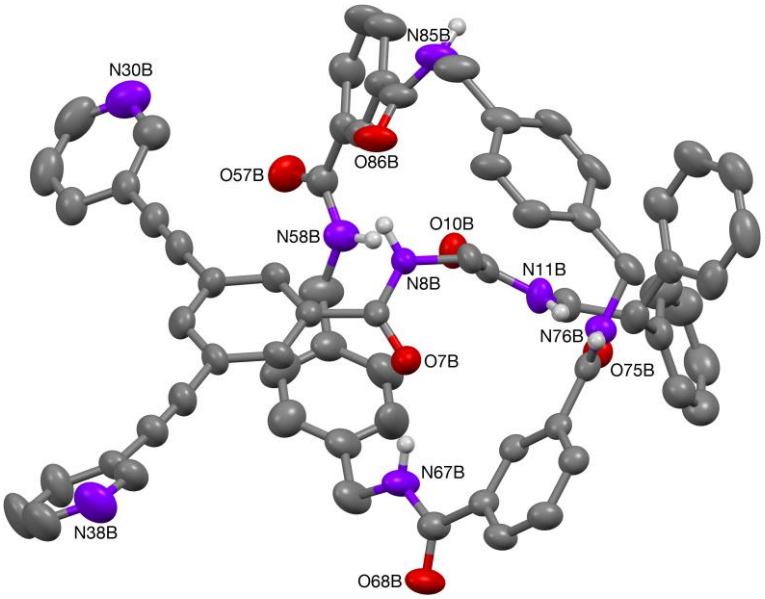

Figure S41 The structure of one (**1-B**) of the two independent [2]rotaxanes present in the crystal of **1** (50% probability ellipsoids).

References

[1] D. S. Marlin, D. G. Cabrera, D. A. Leigh and A. M. Z. Slawin, *Angew. Chem. Int. Ed.*, 2006, **45**, 77.

[2] M. D. Hanwell, D. E. Curtis, D. C. Lonie, T. Vandermeersch, E. Zurek and G. R. Hutchinson, *J. Cheminform.*, 2012, **4**, 17.

[3] A. K. Rappé, C. J. Casewit, K. S. Colwell, W. A. Goddard III and W. M. Skiff, *J. Am. Chem. Soc.*, 1992, **114**, 10024-10035.

[4] J. J. P. Stewart, *J. Mol. Model.*, 2007, **13**, 1173-1213.

[5] Gaussian 16, Revision C.01, M. J. Frisch, G. W. Trucks, H. B. Schlegel, G. E. Scuseria, M. A. Robb, J. R. Cheeseman, G. Scalmani, V. Barone, G. A. Petersson, H. Nakatsuji, X. Li, M. Caricato, A. V. Marenich, J. Bloino, B. G. Janesko, R. Gomperts, B. Mennucci, H. P. Hratchian, J. V. Ortiz, A. F. Izmaylov, J. L. Sonnenberg, D. Williams-Young, F. Ding, F. Lipparini, F. Egidi, J. Goings, B. Peng, A. Petrone, T. Henderson, D. Ranasinghe, V. G. Zakrzewski, J. Gao, N. Rega, G. Zheng, W. Liang, M. Hada, M. Ehara, K. Toyota, R. Fukuda, J. Hasegawa, M. Ishida, T. Nakajima, Y. Honda, O. Kitao, H. Nakai, T. Vreven, K. Throssell, J. A. Montgomery, Jr., J. E. Peralta, F. Ogliaro, M. J. Bearpark, J. J. Heyd, E. N. Brothers, K. N. Kudin, V. N. Staroverov, T. A. Keith, R. Kobayashi, J. Normand, K. Raghavachari, A. P. Rendell, J. C. Burant, S. S. Iyengar, J. Tomasi, M. Cossi, J. M. Millam, M. Klene, C. Adamo, R. Cammi, J. W. Ochterski, R. L. Martin, K. Morokuma, O. Farkas, J. B. Foresman, and D. J. Fox, Gaussian, Inc., Wallingford CT, 2016.

[6] M. Holz, X. Mao, D. Seiferling and A. Sacco, *J. Chem. Phys.*, 1996, **104**, 669.

[3] SHELXTL v5.1, Bruker AXS, Madison, WI, 1998.

[4] SHELX-2013, G.M. Sheldrick, *Acta Cryst.*, 2015, **C71**, 3-8.

[5] A.L. Spek (2003, 2009) PLATON, A Multipurpose Crystallographic Tool, Utrecht University, Utrecht, The Netherlands. See also A.L. Spek, *Acta. Cryst.*, 2015, **C71**, 9-18.